Design, Numerical Analysis and Development of Portable Defogger Duct for Road Vehicles

By

BorifanTadesseTolcha

A Thesis Submitted to Department of Mechanical Engineering

School of Mechanical, Chemical and Materials Engineering

Presented in Partial Fulfillment of the Requirement for the Award of the Degree of Master of Science in Automotive Engineering

Office of Graduate Studies

Adama Science and Technology University

November, 2022

Adama, Ethiopia

Design, Numerical Analysis and Development of Portable Defogger Duct for Road Vehicles

By

Borifan TadesseTolcha

Advisor: Dr. Ramesh BabuNallamothu

A Thesis Submitted to Department ofMechanical Engineering

School of Mechanical, Chemical and Materials Engineering

Presented in Partial Fulfillment of the Requirement for the Award of the Degree of Master of Science in Automotive Engineering

Office of Graduate Studies

Adama Science and Technology University

November, 2022

Adama, Ethiopia

DECLARATION

I hereby declare that this Master Thesis entitled **"Design, Numerical Analysis and Development of Portable Defogger for Road Vehicles"** is my original work. That is, it has not been submitted for the award of any academic degree, diploma, or certificate in any other university. All sources of materials that are used for this thesis have been duly acknowledged through citation.

______________________	______________________	______________________
Name of the student	Signature	Date

RECOMMENDATION

We, the advisors of this thesis, hereby certify that we have read the revised version of the thesis entitled **“Design, Numerical Analysis and Development of Portable Defogger for Road Vehicles**” prepared under guidance by BorifanTadeseTolcha submitted in partial fulfillment of the requirements for Master of Science in automotive engineering. Therefore, we recommend the submission of revised version of the thesis to the department following the applicable procedures.

Dr. Ramesh BabuNallamothu

Advisor	Signature	Date
______________	____________________	________________

APPROVAL PAGE of M.Sc Thesis

I/We, the advisors of the thesis entitled "Design, Numerical Analysis and Development of Portable Defogger for Road Vehicles" and developed by Borifan Tadese Tolcha; hereby certify that the recommendation and suggestions made by the board of examiners are appropriately incorporated into the final version of the thesis.

Major Advisor	Signature	Date

We, the undersigned, members of the Board of Examiners of the thesis by BorifanTadeseTolcha have read and evaluated the thesis entitled "Design , Numerical Analysis and Development of Portable Defogger for Road Vehicles" and examined the candidate during open defense. This is, therefore, to certify that the thesis is accepted for partial fulfilment of the requirement of Master of Science in Automotive Engineering.

Chairperson	Signature	Date
Internal Examiner	Signature	Date

External Examiner Signature Date

Finally, approval and acceptance of the thesis is contingent upon submission of its final copy to the Office of Postgraduate Studies (OPGS) through the Department Graduate Council (DGC) and School Graduate Committee (SGC).

Department Head	Signature	Date
School Dean	Signature	Date
Office of Postgraduate Studies, Dean	Signature	Date

ACKNOWLEDGMENT

I would like to acknowledge and give my warmest thanks to my supervisor (Dr. Ramesh Babu) who made this work possible. His guidance and advice carried me through all the stages of writing my thesis. I would also like to thank my friends and family who have supported me and provided me with great insight into my research.

Finally, I would like to thank the fact that this MSc. thesis would not have been possible without the support of the software. Thanks to my friend Mr. GarbeChukuluJarso (PhD Candidate) for providing an excellent guidance on the ANSYS Fluent solver software.

TABLE OF CONTENTS

CONTENTS **PAGES**

LIST OF FIGURES

LIST OF TABLES

LIST OF ABBREVIATIONS

FEA	Finite element analysis
ANSYS	Analysis Systems
CATIA	Computer Aided Three-Dimensional interactive application
CFD	Computational Fluid Dynamics
FMVSS	Federal Motor Vehicle Safety Standards
PVC	Polyvinyl chloride
DLAS	Diode laser absorption spectroscopy
UPEM	Ultrasonic pulse-echo method
PBI	Poly Benz imidazole
SAE	Society of Automotive Engineering
AC	Air Conditioning

NOMENCLATURE

A	Windshield area, [m^2]
f t	Thickness of water film
D	Factor of mass transfer
E	Energy, [J/kg]
g	Gravitational acceleration, [m/s^2]
$\hat{g}$	Density of moisture flow, [kg/m^2 s]
h	Convective heat transfer, [W/m^2 K]
$\hat{h}$	Sensible enthalpy, [J/kg]
I	Unit tensor
K	Thermal conductivity, [W/mK]
m	Mass, [kg]
p	Static pressure, [Pa]
Q	Heat flux, [W/m^2]
T	Temperature, [K]
V	Velocity vector

Greek Symbols

Θ	Evaporation factor, [kg/m^2h]
P	Density, [kg/m^3]
T	Stress tensor

Indices

a	Air
e	Equivalent
g	Glass
w_o	Outward surface of windshield
f	Vapor film

ABSTRACT

Formation of the fog on windshield and window glasses obstructs the visibility of the drivers. A defogger is used in cars to remove ice or condensation from the window glass. The objective of this thesis is to designs and performs a numerical analysis of the portable side and windshield glass window defogging of an automobile. As part of this work, the defogger duct nozzle is built utilizing stated boundary conditions for vehicle defrosting in a lab experiment which uses recommended exit port air speed according to Federal Motor Vehicle Safety Standards (FMVSS) in the United States and the Society of Automotive Engineering SAE. The simulation begins with a portable duct layout that equally distributes the flow in the exit port at a speed of 6 m/s. K-epsilon turbulence model is used in duct flow design to mimic cold air with steady-state performance. The final form of the duct nozzle is used as the primary design. The duct design is later finished, and a full-scale Toyota HIECE 2004 quarter model is used to study numerical simulation of the automotive defogs process. An Eulerian wall film multiphase flow model from ansys fluent is used to carry out the simulation. The average non-movable liquid water film thickness of 315.4µ m and 337.2 µm based on measurements made using the ultrasonic pulse-echo technique (UPEM) and diode laser absorption spectroscopy, respectively, is applied to the window glass in accordance with experimental results from prior work. In order to replicate film thicknesses of 1.4mm, 1.05mm, 0.7mm, and 0.35mm, hot air velocity is pumped from the exit part of a duct to the film surfaces on the glass windows. The distinctive output parameter predicted here is the volume percentage of the water film that changed after a particular flow interval. The defogging performance simulation needs 1500, 2500, 3000, and 3500 seconds for each of the four possible film thicknesses, respectively, to clear the surface of all condensed water. Finally, obtaining a quick defogging time that prevents the ice from the surface is the greatest alternative for this research. Therefore, the 0.35mm 1500 second time delay film is a carefully chosen film thickness for a highly portable defogger machine for three windows. To develop a portable defogger with minimal energy consumption that gets its power from a solar panel or alternator via a battery. The designee chose the heater, fan, and battery sizing after 1500 seconds. A prototype has been developed for exhibition and operational testing made based on the final defogger duct nozzle and component sizes. Finally, the functional tested prototype takes around 1420 second which is reliable with the numerical obtained defogging time which consumes 2kw power with 1500 seconds that can all widows' surfaces dries.

Keywords: *Defogging, Evaporation, Fogging, Window glass, Droplet*

CHAPTER ONE
INTRODUCTION

1.1 Background

The presence of fog on the windshield glass reduces or sometimes blocks the driver vision which may endanger the driver as well as other drivers in the road. Windshield fogging is also a frequent problem occurring in the car due to condensation of water vapor on the glass and would be the result of two phenomena: (1) Decreasing the glass temperature below the dew-point temperature, (2) Increasing the humidity ratio in the vehicle compartment. This is always due to more humidity inside the car than outside, as the human occupants emit humidity via perspiration and respiration (breathing). In the small confines of an automobile, especially in case of maximum occupancy, the relative humidity inside can quickly reach 100%, Taro Ono et al (2019).

Windshields fog up because of differences in temperature and moisture in the air humidity. Window fog is caused by moist, humid air inside the vehicle meeting the cold windshield before it’s warmed up. There are several factors contributing to this humid air: Driver or passenger breathing / inhaling and exhaling, a steaming mug of coffee, the rain and snow on passenger clothes etc. The humid/moist air meets the cold surface of the windshield glass, releases moisture, and condenses into a fog. The key to whether to find a fog is the temperature at which the maximum amount of water vapor can be held in the air at a given pressure before condensing into a liquid. This is known as the dew point. The air trapped in the car from the previous day will be more humid than the outside humidity level, therefore holding more moisture, A Ene, C Teodosiu (2021).

The present work contains the conducted a numerical analysis of portable defoggerfor side window glass and windshield defogging process of an automobile. The analysis has been carried out for micro level droplet and maximum droplet size to investigate the performance of the defogger numerically. And ThePrototype of portable defogger is prepared for demonstration of its functionality.

1.2 Statement of problem

Fogging problems on the windshield interior are the most common problem when temperatures are near freezing or in humid conditions A Ene, C Teodosiu (2021).Depending on climate conditions in their locations, some agencies may experience fogging more often and more severely than others. In addition to ambient humidity, other moisture in the cab can contribute to fogging, including melted snow from the operator’s boots and moisture from his breathing. Fogging is less of a problem at very low temperatures. The water is "frozen out" of the air when it is too cold to keep enough water vapor to cause a condensation issue on the windshield. To solve this problem, the drivers expected to open the windows, the vehicle air conditioner (AC) of vehicles, and some chemical and portable defogger to remove the fog from the front of the windshield as Taro Ono et al (2019),.

Some drivers using AC to defog the humidity in vehicles need AC gas, which is very expensive. Therefore, some drivers use portable defoggers and chemicals. And also the portable defogger has a large size and uses vehicles' batteries through cigarette ports W. Yang, et al (2012). A method of defogging using a vehicle battery’s defogger reduces the battery’s performance.

Therefore, the scientific contribution on this research is to optimize the shape of defogger duct based on numerical analysis which is used for all windows in cabins or drivers sides.

1.3 Objectives

1.3.1 General Objective

The general objective of this thesis work is to Design and analyze a Portable defogger duct for windshield and side window glasses of vehicle.

1.3.2 Specific Objectives

The specific objectives of the proposed project are as follows

- To design the physical size and shape of the defoggerduct.
- To develop the 3d model of defogger
- To analyze designedsize of defogger duct and its performancenumerically
- To prepare prototype for demonstration purpose and its functionality test.

1.4 Significance of the Project

- Reduces defogging system maintenance time
- Reduces overall cost
- Reduces wear of components
- Increases reliability
- Improves defogging ability
- It helps in using Solar energy

Scope of the Study

The study focus on design of portable defogger Duct arrangement with vehicle window and. This work have study concerning to different concept of duct by using Computational fluid Dynamics software.

Basically the study focused on;

- Designing and Sizing Portable duct using Ansys Fluent Solver
- The study also contain the numerical defogging simulation of car window
- Physical prototype is developed for testing its functionality.

1.5 Organization of the Thesis

In this research, the thesis work is organized into the following chapters. Chapter one describes a general introduction of the Thesis. Chapter two presents a literature review of the existing defogging system of the vehicle. Chapter Three describes materials and methods to be used together with general boundary conditions of numerical techniques. Chapter four covers the result and discussion of numerical analysis. Chapter five comprises calculations for sizing different electrical and fluid flow components and prototypes. Chapter six is about Summary and Conclusion with both future work and recommendation.

CHAPTER TWO
LITERATURE REVIEW

2.1 Introduction

One of the vital performances in vehicles HVAC systems is demist/defrost. In addition to safety associated with improved defrost and demist performance. Applying high temperatures for defogging is usually avoided as it may reduce the driver's alert.

2.2 Types of defogger

2.2.1 Primary defogger

For primary defogging, heat is generally provided by the vehicle's engine coolant via the heater core; fresh air is blown through the heater core and then ducted to and distributed over the interior surface of the windshield by a blower. This air is in many cases first cooled down and dehumidified by passing it through the vehicle's operating air conditioning evaporator. Such dehumidification, when followed by a reheating, makes the defogging more effective and faster, for the dry warm air has a greater capacity of absorbing water from the glass at which it is directed (with respect to the moist warm air provided by the heater alone, and the dry cold air provided by the air conditioning system alone). However, whenever the vehicle is equipped with an air conditioning system, care must be taken to keep it in an operational state for the primary defogger to operate optimally. Also, at very low ambient temperatures, the air conditioning system might not turn on, in order to prevent possible compressor damage. In modern vehicles, running this type of defogger often automatically switches the air conditioning system on, without further action required (FMVSS 103) Manuel Lorenz (2015).

2.2.2 Secondary defogger

Secondary defoggers, such as those used on a vehicle's back glass and/or side view mirrors, often consist of a series of parallel linear resistive conductors in or on the glass. When power is applied, these conductors heat up, thawing ice and evaporating condensation from the glass. These conductors may be composed of a silver-ceramic material printed and baked onto the interior surface of the glass, or may be a series of very fine wires embedded within the glass. The surface-printed variety is prone to damage by abrasion, but can be repaired easily with a conductive paint material. Federal Motor Vehicle Safety Standard (FMVSS 103) requires all passenger cars, multipurpose passenger vehicles, trucks, and buses manufactured on or after January 1, 1968, to have windshield defrosting and defogging systems. However, rear window defrosting and defogging systems, hereafter referred to as rear window defoggers, are not required. Rear window defoggers became available as optional or standard equipment in most cars during the 1970's or 1980's and are popular with consumers. Rear window defoggers allow the driver to see through the rear window under adverse weather conditions. Clear vision is especially important when the driver wants to back up or change lanes.

FMVSS 104 requires all passenger cars, multipurpose passenger vehicles, trucks and buses manufactured on or after January 1, 1968, to have windshield wiping and washing systems. Similar to rear window defoggers, rear-window wiping and washing systems are not required. Rear window wipers have been installed on a smaller group of vehicles for even better vision.

This study assesses the effectiveness of rear window defoggers in reducing crashes in which a driver is backing up, changing lanes, or performing other tasks that would be facilitated by vision through the rear window. Typically, studies to assess the effectiveness of a vehicle safety standard consist of an analysis of crash data that compare the experience of vehicles that meet the safety standard to those that do not meet the standard. For most evaluation studies, we can identify exactly what vehicles were equipped with a safety technology, and which ones were not, based on the model year (e.g., before/after a standard's effective date, or before/after a date when the technology became standard equipment) or dedicated VIN characters (e.g., air bags), or specific mention in the crash data (e.g., child safety seats). However, rear-window defoggers and wipers have never been required safety equipment and were offered as optional equipment, for many years, on quite a few make-models. The presence of rear-window defoggers and wipers generally cannot be deduced from the first 12 characters of the VIN, and it is rarely (if ever) mentioned on crash data files. Therefore, it is necessary to obtain information on the proportion of vehicles with rear-window defoggers or wipers from another source of FMVSS 104.In the absence of a better solution, snowplow operators may remove fog from the windshield with a rag, towel or even their sleeves or hands, but this can be a dangerous distraction during plowing, and operators cannot generally reach all interior glass surfaces comfortably from the driver's seat. Removing fog this way can cause streaks and smears on the windshield, and the fog will continue to reappear unless conditions inside the cab change. Figure 2.1 shows Schematic diagram of windshield fog.

Figure 2.1.Schematic diagram of windshield fog (FMVSS 104)Manuel Lorenz (2015).

One respondent mentioned that windshield and side window fogging occur often when the operator uses the defrost/floor heat setting (so the ventilation system is running the defroster and floor heat at the same time).

Two approaches found to be effective in combating interior fogging, which may be used simultaneously, are to increase airflow over the windshield and to reduce the moisture content in the air. Some agencies mount small fans inside the cab to direct air over sections of the windshield or windows that do not receive adequate airflow from the truck's ventilation system. To dry the air, agencies may use an air conditioner, alone or as part of the systems defrost setting. In vehicles without air conditioning, the defrost setting circulates warmed air from outside across the windshield from FMVSS 103.

2.3 The different parameter to windshield defogger

2.3.1 Adding fans to increase airflow over windows

Several companies offer aftermarket automotive fans that can be mounted on the vehicle's dashboard or on the interior roof of the cab near the top of the windshield. They may plug into a 12-volt outlet such as the cigarette lighter, or be wired into the vehicle's electrical system. Operators can position these fans to increase airflow to any areas of the windshield that are not served adequately by the vehicle's ventilation system. Survey respondents were familiar with the practice of adding fans to increase airflow. Most were aware of it, and 51% reported that their drivers had used this strategy to combat interior fogging. Survey respondents reported that improvements in the ventilation systems on newer trucks, including the presence of air conditioning, more blowers that are powerful, better vent placement and improved overall efficiency, have reduced the need for auxiliary fans. "These systems work better than past equipment and we are finding our personnel are not using the auxiliary fans," said one respondent.

2.3.2 Using air conditioning to dry the air

Air conditioning compressors remove moisture from the air in the vehicle's cab, thereby minimizing condensation and fogging on the windshield and windows. The compressor may also be engaged during the ventilation system's defrost cycle. Many respondents were aware that air conditioning can be used to combat interior fogging, but only 23% had used this strategy. Two respondents expressed concerns about the effectiveness of using air conditioning to combat fogging. One said that using air conditioning to move warm air was not effective because not enough air comes through the defroster vents "and you completely lose the windshield." As mentioned, not all agencies have used air conditioning to combat interior fogging, and many do not have air conditioning on their maintenance trucks; it may not have been available on older trucks, and not all agencies specify it when ordering a new truck according to FMVSS 103.

2.3.3 Turning off heat to keep windshield cold

Another strategy for eliminating fogging is to minimize the temperature difference between the inside of the cab and the outside air, which also minimizes the humidity difference and the opportunity for condensation to form on the windshield. The primary disadvantage to this strategy is the issue of driver comfort, which is a distraction that may compromise safety and effectiveness must note by FMVSS 103.

2.3.4 Adding aftermarket windshield heaters

Heating the windshield using aftermarket heaters is another strategy for addressing fogging that we identified during our pre-survey research. Heating the windshield decreases the temperature differential between the air in the cab and the windshield, which inhibits the formation of condensation on the windshield note by FMVSS 103.

2.3.5 Chemical glass treatments

Several companies make liquid glass treatments that repel moisture. A few respondents reported using sprays or rub-on liquids, and Rain-X makes anti-fog towelettes and anti-fog glass cleaner wipes specifically for interior windshields note by FMVSS 103.

2.3.6 Other solutions

The double-paned windshield interior fogging as well as exterior icing. By insulating the interior windshield from the cold outside air, the interior glass stays nearer to the same temperature as the air inside the cab, minimizing condensation note by FMVSS 103.

A new design for the defrost system of Jaguar Land Rover with one inlet panel at the bottom of the windshield was proposed by Karamjit S et al (2011). His aims in his study were to achieve the correct air flow distribution of about 1.5-2 m/s across the windscreen Karamjit S et al (2011).

As demonstrated by Zolet et al (2011) the defogging simulation methodology developed by FIAT Brazil and Multicorpos Engineering. They used CFD simulations with Star CCM+ software. Experimental data obtained from climatic chamber was used to compare their numerical data and validate the methodology.

Croce, G et al (2007) Simulated defogging procedure in the windshield. In their simulation, the water layer was considered as a collection of closely packed tiny droplets, leaving a portion of dry area. They considered the effect of the contact angle.

R.B. Kharat et al (2007) developed a model which accounted for whole cabin climate changes to predict the process of fogging and defogging based on program C. This model can offer a relatively accurate analysis for the fogging process.

The HVAC (Heating, Ventilation, and Air Conditioning) systems currently consume a significant amount of energy Jixuan Liu et al 2016. The model was developed based on the three thermodynamic balances; mass balance, moisture balance, and energy balance. Adding a very thin air layer near to the glass surface to demonstrate the temperature gradient of glasses and the fogging process.

There are some researches in the literature concerning simulation and prevention of mist formation phenomenon in other fields like supermarket refrigerators Himanshu, K et al (2014).

Most of the works in the mentioned field deal with achieving velocity field in the compartment while simultaneous consideration of both velocity and temperature fields, is little accomplished in the literature. As mentioned before air moisture content is the main issue for the mist/frost formation on the windscreen. Heating acts to lower the relative humidity of the air, but as long as the glass remains cool there will still be condensation forming. To halt the condensation, heating must be applied long enough to warm up the glass itself above the dew point of the interior air. Furthermore, heating the glass causes the interior of the car to be overheated and consequently the passengers come up with uncomfortable conditions.

2.4 Review of Related literature on Computational fluid dynamics

S. J. KANG .et al (2016)has done numerical analysis of automobile defrosting system through a full-scale mode computed by a finite volume computational fluid dynamics (CFD) program and experimental investigations for validation of the numerical results. The method used to solve is, Air is chosen as the flow medium, and its physical properties are chosen at ambient conditions. The initial temperature of the compartment and windshield is − 6.9°C. The defroster grillers are employed to inject the air at a velocity of 14 m/s with an injection angle of 45 degrees. The injection angle (θ) may be defined as the angle between the windshield and the incoming flow from the defroster nozzle. The unsteady inlet temperature varied from −4.2°C to 40.7°C as the initial and final temperature, respectively, over a period of 30 minutes. Fixed static pressure is selected for the outflow condition. For the boundary condition, the whole compartment except the windows and windshield is assumed to be adiabatic. The ambient temperature is considered to be −6.9°C and isothermal. The result founded that the airflow produced by the defrost nozzle is highly no uniform in nature and does not cover the whole windshield area. The no uniformity also severely affected the heating temperature pattern on the windshield. The windshield temperature reached a maximum in the vicinity of the defroster nozzle in the lower part of the windshield and ranged from 9~31°C over a period of 30 min, which caused the frost to melt on the windshield. The melting time was under 10 minutes, which satisfied the NHTSA standard. The numerical predictions were in close agreement with the experimental results. Thus, he concludes that CFD can be a very useful design tool for an automobile HVAC system.

Zhilong He et al (2020) Studied Analysis and Optimization of Truck Windshield Defroster. He studied for Frosting and fogging of automobile windshields is a common problem that emerges in daily driving. It is important and essential to quickly and completely defrost the windshield for safety purposes. In this study, a three-dimensional mathematical model has applied to investigate the flow distribution and flow characteristics on the windshield of a medium-size Model N800 truck. Three boundary conditions have defined: inlet boundary, outlet boundary, and windshield surface boundary conditions. Inlet boundary condition: the velocity inlet boundary condition (velocity-inlet) is used, and the inlet speed is determined according to the flow rate of the blown surface and the defroster duct inlet area. The inlet air temperature is introduced according to the Heating, Ventilating and Air Conditioning (HVAC) heating curve. And the initial temperature was 253 K. The HVAC heating curve is measured during the experiment. (2) Outlet boundary condition: a pressure outlet (pressure-outlet) was applied. The pressure at the outlet is equal to the working pressure (101.325 kPa). (3) Windshield surface boundary condition: the glass surface is defined as a stationary wall, and the initial temperature condition of the glass surface was 255 K. The initial thickness of frost was set to 1 mm. The simulation results are first compared with experimental data. The results showed that the simulation model could reliably predict the defrosting performance on the windshield. This model is then used to optimize the design of the defrosting duct that comprised the main part of the defroster. It is found that the guide plate and outlet position of the defrosting duct is the two major factors affecting the defrosting performance. Therefore, the guide plate is first optimized and the defrosting performance is analyzed. The results showed that the average pressure loss dropped by 21.56%, while the defrosting efficiency at the front white zone was improved to 89%. The position of the outlet of the airflow was further studied. The results showed that the defrosting efficiency at the front zone could be further improved to 99%.

Maciej et al (2020)conducted the research onEfficiency of electric vehicle interior heating systems at low ambient temperatures. Along with the development of vehicles, the technology used in their construction also changes. The biggest calls at the moment are batteries for vehicles, as well as their ranges on a single charge. There are already vehicles with ranges of 500 km or even 600 km. However, it turns out that these are not the only problems with electric vehicles One of the drawbacks is the way they heat their passenger cabins. There is no typical heater in an electric vehicle as in the case of a vehicle with a conventional drive. For this purpose, e.g. an electric heater with a blower is used for this purpose. For this reason, the authors of this paper decided to determine the efficiency of the heating system in an electric vehicle at low ambient temperatures. Own tests were carried out on the vehicle at temperatures of +5∘C, −5 ∘C and −10∘C. Based on the research, the authors of the paper could draw conclusions on how to heat the interior in the electric vehicle under test, as well as check whether the efficiency of such a system for individual places in the car is sufficient to obtain the set temperature. For more information, the following figure 2.2 shows graph of the vehicle air conditioning heating system.

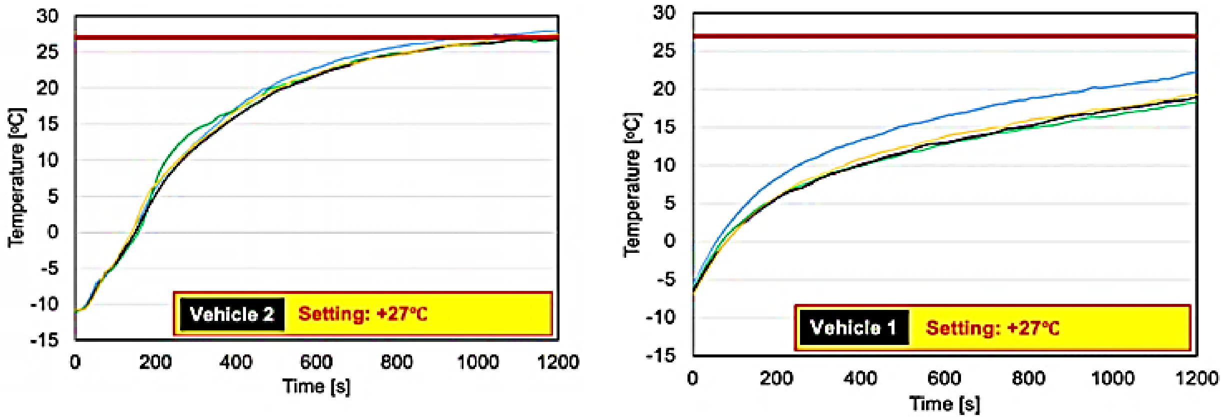

Figure 2.2.The process of heating the interior in car 2 &1 for air-conditioning setting of +27◦C &27ºC and ambient temperature of −5 ◦C & -10ºC prospectively;Maciej et al (2020)

Arafat A et al (2017). Study, the developments of 3D wall filming mechanism for coal combustion in a small scale furnace under air and oxy-fuel combustion conditions are obtainable. His study is to develop the film flow behavior and particle deposition characteristics on the furnace refractory wall using a commercial CFD code coupled with some user-defined sub-routines. Eulerian-Lagrangian approach of the gas-particle flow is coupled with the particle-wall interaction mechanisms including particle capturing, entrainment and wall burning sub-models. The presentation contains to validate the model in a small scale furnace by comparing the available temperature, species data for coal-water slurry combustion and reasonable agreement has been observed. Visualization of the transient film formotion and flow characteristics under air and oxy-firing cases are presented. The film thickness deposited on the refractory wall is found to be reasonably in good range with the available data. The deposited film thicknesses for both the conditions are found in the range of 0–1.0 mm. The average molten film velocity was 0.0001 m/s due to higher viscosity and greater surface tension properties. Slightly higher amount of films are formed in oxy-firing condition due to slower char oxidation rate.

Hyu-Goo Kang et al (2008) worked ondefrosting performance on automobile Windshield through different injection angle to find out the most effective injection angle for deicing through SC/Tetra, a commonly used CFD software. For its visibility is one of the most important phenomenon. The primary factors which affect the efficiency of deicing are 3D geometry of Defrost Nozzle, the inlet velocity and temperature of the flow and the injection angle. However, in his paper, all these parameters are optimized by changing the injection angle. A wide range of injection angle from 5 degree to 50 degree has been measured for analysis. A very good defrosting performance has been achieved with 45^{o} degree injection angle which can satisfy the condition of National Highway Traffic Safety Administration (NHTSA).

Based on researcher method of analysis for Control factor to evaluate the effect of on defrosting and dehumidification functions, ten different models (from 5 to 50 degrees) shown in fig. below are used to figure out the efficiency and the ideal angles of air blown to the windshield for defrosting and dehumidification. The Ɵ is from sprinkled angle of the air from the nozzle. Figure 2.3 shows defogging angle with windshield surface

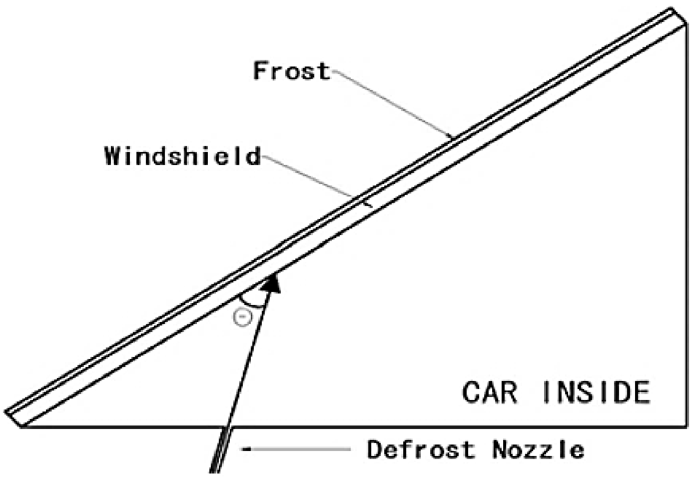

Figure 2.3.Defogging angle with windshield surface;Arafat A et al (2017)

The performance test provision function of defrosting and dehumidification on the windshield is essential and the regulated object. The following figure 2.4 shows the Vision areas on the windshield classified by A, B and C. on this study.

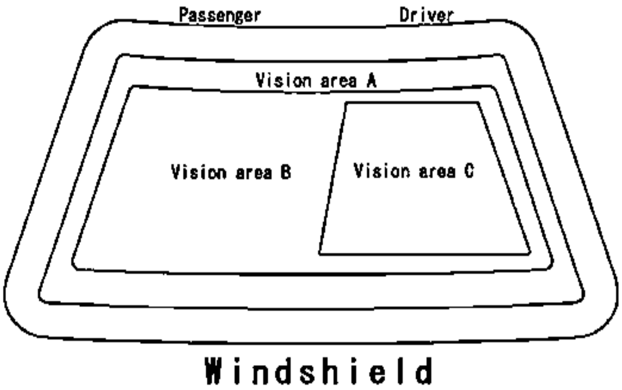

Figure 2.4.Vision areas on the windshield classified by A, B and C;Arafat A et al (2017)

For in major developed countries, the function of defrosting is compulsory to defrost the definite section on the windshield within a few minutes after starting an engine by law regulating, for example, NHTSA & MVSS103, the U.S authorization, ECC, Europe authorization Fig. above shows the visibility on the windshield. In the authorization, MVSS103, after sprinkling some water on the windshield and leaving 30 through 40 minutes in -20℃ to generate frosts, the Vision area C is regulated to remove it's 80% or more within 20 minutes and the Vision area A is regulated to remove 95% or more within 45 minutes.

The graph, Figure 2:5is about how fast the Frost can be defrosted in a certain angle. Relatively, the efficiency of the models that have the wide angle when the air from the Injection nozzle strikes the windshield is better. Most of them, the 45 degree is the most efficient model.

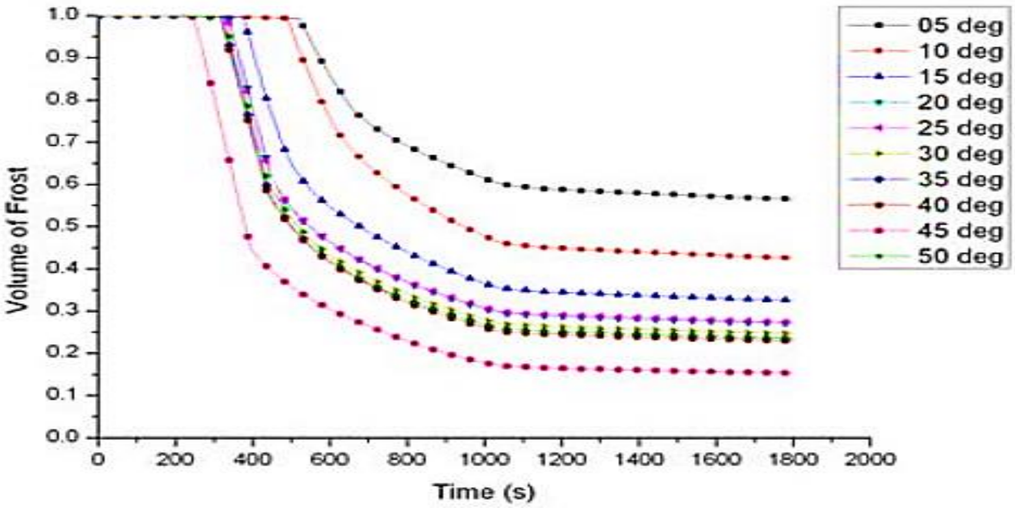

Figure 2.5.Effect of injection angle on the volume of frost; Arafat A et al (2017)

(A) in Figure 2.6, is the picture that shows uniformly spread Frost on the windshield when vehicles start an engine and the air temperature from the Injection Nozzle is -5℃ (B) is the picture that shows the process of the defrosting when in 5 minutes after starting the experiment. (B) Also shows the progress of the sections both Vision area B and Vision area C when the temperature became 11. The picture, (C) shows the process of the defrosting when in 7 minutes. The sections both Vision area B and Vision area C have been almost defrosted but Vision area A has remained much more Frost. The picture (D), when in 12 minutes shows that every section has been defrosted except the heat transfer untouched area so that it meets the authorization, Figure 2.6 melting pattern of frost

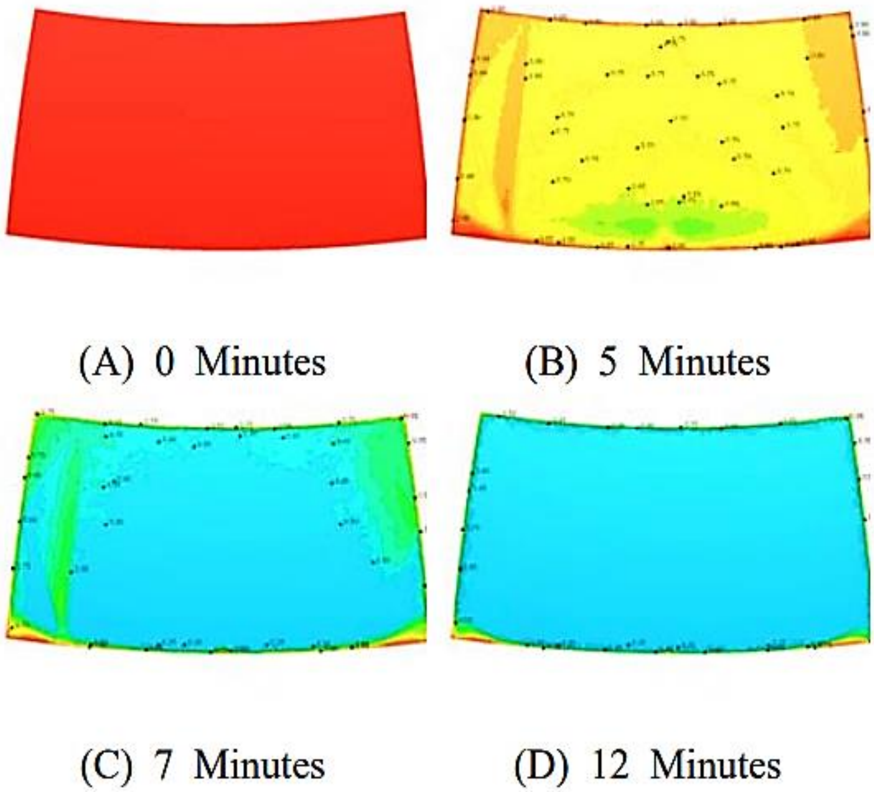

Figure 2.6.The melting pattern of Frost with respect to time;Arafat A et al (2017)

Dohyung Kim et al (2019) Conducted the research on Improvement of Defogging Performance of Automobile Defroster using Vortex Generators Fog on the automotive windshield interferes with the sight of the driver and causes serious safety problems; thus, removing it rapidly has been a longstanding goal in the automobile industry. In his study, the novel method for improving the defogging performance of the defroster without its structural alteration by using vortex generators (VGs). To optimize the performance of the VGs, he performed particle image velocimetry experiments, an evaporation measurement experiment, and a numerical simulation for visualizing the airflow from the defroster inlet. The dimensions of the VG (height $h = \delta$ and length $\ell = 5\delta$) were selected according to the boundary-layer thickness, δ, of the lowest-flow rate ($u_{low} = 0.33$ m/s) used in the defroster inlet. dimensionless parameter, i.e., the secondary flow intensity (Se), to quantify the intensity of vortices for several angles of attack (30°, 45°, and 60°). The results indicated that the vortices generated from VGs with a 30° angle of attack retained their maximum intensity until they reached the vision area of the driver. Additionally, he explored two different configurations of VGs—co-rotating and counter-rotating—and concluded that the counter-rotating configuration had higher performance than the co-rotating configuration. The optimized VGs were directly inserted in the defroster inlet and improved the defogging performance by approximately 10%. Finally the conclusion is, the method is can be applicable to various automobile models for enhancing the performance of the defroster regardless of the interior volume, air-ventilation performance, and other conditions, such as the number of passengers and outside temperature. Figure 2.7 shows VGs.

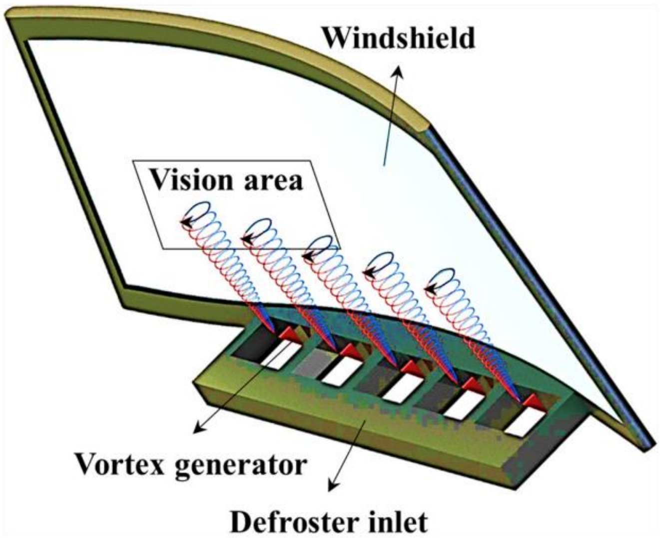

Figure 2.7.Concept of defogging performance enhancement of the defroster with VGsDohyung Kim et al (2019).

Finally, the embedded 50 VGs inside the defroster inlet of an actual automobile (Santa Fe, Hyundai Motor Company), and evaluated the enhancement of defogging performance due to the VGs. The VGs were modeled using commercial computer-aided design software (SolidWorks 2015, Dassault)

From simulation, results below the dried area had a high evaporation ratio close to 1 (red), whereas the fully wetted area had a low evaporation ratio value close to 0 (blue). The red solid line from experimental represents the boundary between the wetted area (dotted area) and the dried area (plane area) figure 2:8 shows Schematic of experiment.

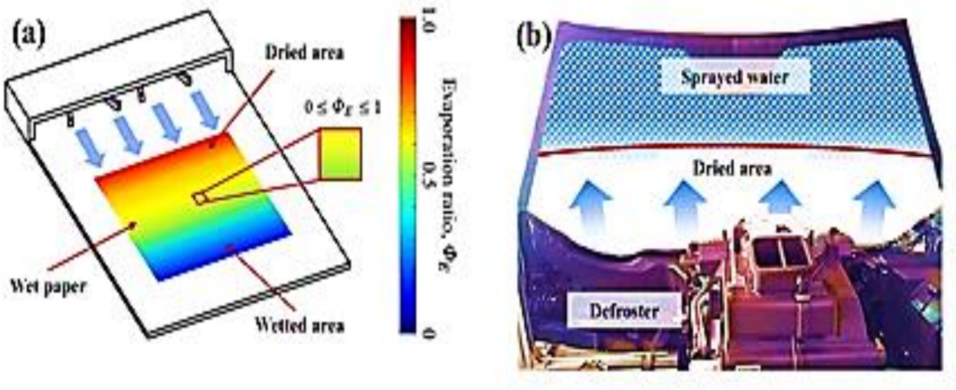

Figure 2.8.(a) Schematic of the wetted-paper experiment (b) Experimental setup for measuring the defogging performance of the VG-embedded defroster inlet; Dohyung Kim et al (2019).

Huinan Yang, et al (2018) Studied Measurement of liquid water film thickness on opaque surface with diode laser absorption spectroscopy. On this research work, a novel on-line measurement method based on diode laser absorption spectroscopy (DLAS) is developed to determine the film thickness on opaque surfaces. The evaporation process of static liquid films both on a silver-coated mirror (smooth opaque surface) and an aluminum alloy plate (rough opaque surface) were investigated with the proposed method. Ultrasonic pulse-echo method (UPEM) is simultaneously applied to validate the measurement accuracy of DLAS method, it revealed that the average thickness deviation between these two methods during film evaporation process on silver-coated mirror were 4.9% and on aluminum alloy plate were 7.1%, respectively. A flow liquid film on aluminum alloy surface is then studied, it is found that the average thickness deviation between DLAS and UPEM at low flow speed was 6.5% and at higher flow speed was 9.5%, respectively. In addition, the fluctuation frequency of the liquid film at both flow speeds was in good agreement with these two methods. The case of low flow velocity, the average film thickness is 315.4 µm and 337.2 µm by DLAS and UPEM, respectively, the average fluctuation amplitude of the dynamic water film is about 93 µm and about 105 µm by DLAS and UPEM, respectively. The DLAS fluctuation frequency of the water film is 13 Hz, it is in good agreement with UPEM.

2.5 Research Gap

The following gap has been drawn from the review of related works.

- Experimentally most, typical fog machines create a fog particle size of 1-5 micron. However, the researchers has done with 1mm thickness that may consume huge amount of energy during defogging period that for primarily, heat is generally provided by the vehicle's engine coolant via the heater core; fresh air is blown through the heater core and then ducted to and distributed over the interior surface of the windshield by a blower. But there is maximum size of droplet which is about 5mm diameter.
- But the highly optimized shape of defogger duct machine should be designed to remove 1mm thickness within the short period of time and also it should remove maximum droplet size of tropical rain fall which is about 5mm.And also the CFD test should be considered for micro level fog which is very good to designee of portable defogger that don't consume huge amount of energy from the electrical sourcesby consideringside window glass and windshield included.
- To solve these gaps the cold flow analysis is made for portable designee of duct and the eulerian film model has been developed to check the portability of defogger during defogging of window glass of different fluid film thickness.

CHAPTER THREE
MATERIALS AND METHODS

3.1 Introduction

For the accomplishment of the set objectives proper required materials are to be used and a step by step systematic methodology has to be followed. The materials selected and methodology has been followed. Because the materials selected and methodology followed are given clearly in this chapters. Thorough out literature survey helped in the proper selection of working materials, research methodology, and simulation software are incorporated. In this study, the designs are carried out byselecting better materials.

3.2 Materials

It is obviously known that a prototype is a replica of a product which is used as an early model to test the product and get feedback from interested party before they can invest in idea. That being said, prototyping is an exhausting and time-consuming practice in product design. Therefore, on this thesis the decision has been made to do the prototype for its functionality purpose and demonstration. There are many materials can be necessary for preparing portable type of defogger machine. The list of materials used are given in table 3.1.

Table 3.1.Materials Used for Prototype

SNo	Name	Quantity	Unit Size
1	Polyvinyl chloride (PVC)	1	2000mm
2	Gypsum (Gesso)	1	1kg
3	Flexible Hose	3	1m
4	Heating Resistor	1	0.3m
5	Spray paint	1	16 fluid ounces (473ml)
6	Lead Acid Battery	1	6v;4.5Ah

3.2.1 Detail of Electrical Materials

Voltage regulator

A voltage regulator is an integrated circuit (IC) that provides a constant fixed output voltage regardless of a change in the load or input voltage. It can do this many ways depending on the topology of the circuit within. For this project the LM338 was used, LM338 are adjustable 3-terminal positive voltage regulators capable of supplying in excess of 5A over a 1.2V to 32V output range. They are exceptionally easy to use and require only 2 resistors to set the output voltage.

Transistor

A transistor is a semiconductor device used to amplify or switch electronic signals and electrical power. Transistors are one of the basic building blocks of modern electronics. It is composed of semiconductor material usually with at least three terminals for connection to an external circuit.NPN transistors are a type of bipolar transistor with three layers that are used for signal amplification. A device is controlled by the current. A negative-positive-negative transistor is denoted by the abbreviation NPN. In an NPN transistor, the flow of electrons is what causes it to conduct.Figure 3.1 show Transistor components.

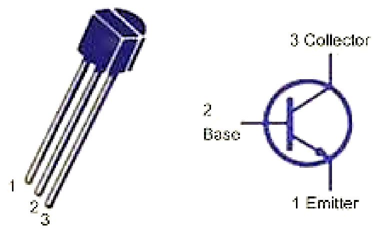

Figure 3.1. Transistor component (https://pnpntransistor.com/transistor)

Resistor

A resistor is a passive two-terminal electrical component that implements electrical resistance as a circuit element. In electronic circuits, resistors are used to reduce current flow, adjust signal levels, to divide voltages, bias active elements, and terminate transmission lines, among other uses. Figure 3.2 is about the specific type of resistor components.

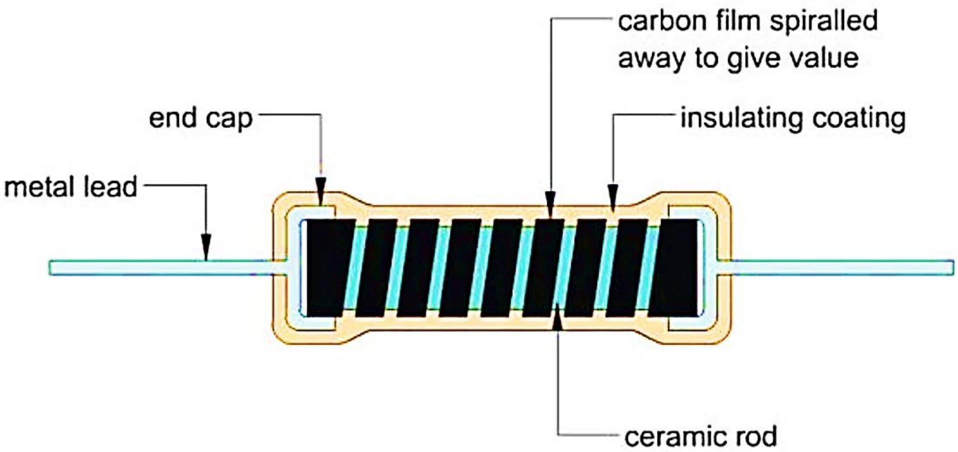

Figure 3.2. Resistor Component (http://denethor.wlu.ca/common/resistors)

Potentiometer

Potentiometers work by varying the position of a sliding contact across a uniform resistance. A potentiometer has the two terminals of the input source fixed to the end of the resistor. To adjust the output voltage the sliding contact gets moved along the resistor on the output side. Figure 3.3 represent the sliding type of potentiometer.

Figure 3.3. Sliding type of Potentiometer (www.phidgets.com)

Diode

1N4007 is a PN junction rectifier diode. These types of diodes allow only the flow of electrical current in one direction only. So, it can be used for the conversion of AC power to DC. 1N 4007 is electrically compatible with other rectifier diodes and can be used instead of any of the diode belonging to 1N400X series. Figure 3.4 is normal diode used on ac to DC convertor.

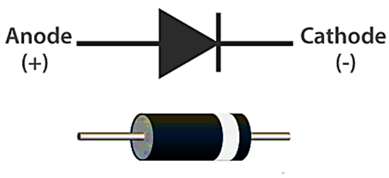

Figure 3.4. Normal Diode (www.electrical4u.com/diode)

Solar panel

Solar panels are those devices which are used to absorb the sun's rays and convert them into electricity or heat. Description: A solar panel is actually a collection of solar (or photovoltaic) cells, which can be used to generate electricity through photovoltaic effect.

Heat resistance plastic

Heat resistant plastics are polymeric materials that are engineered to withstand continuous operating temperatures up to and exceeding 300° F without any negative effect on their mechanical properties. Polybenzimidazole (PBI) has the highest heat and wear resistance, strength, and mechanical property stability of any engineering thermoplastic on the market today. PBI fibers have no known melting point, don't burn, and don't stick to other plastics.

3.3 Methods

In order to address the general and specific objectives of this work a well-designed methodology were followed. The figure 3.5below shows the steps of methodology followed in the form of a flowchart.

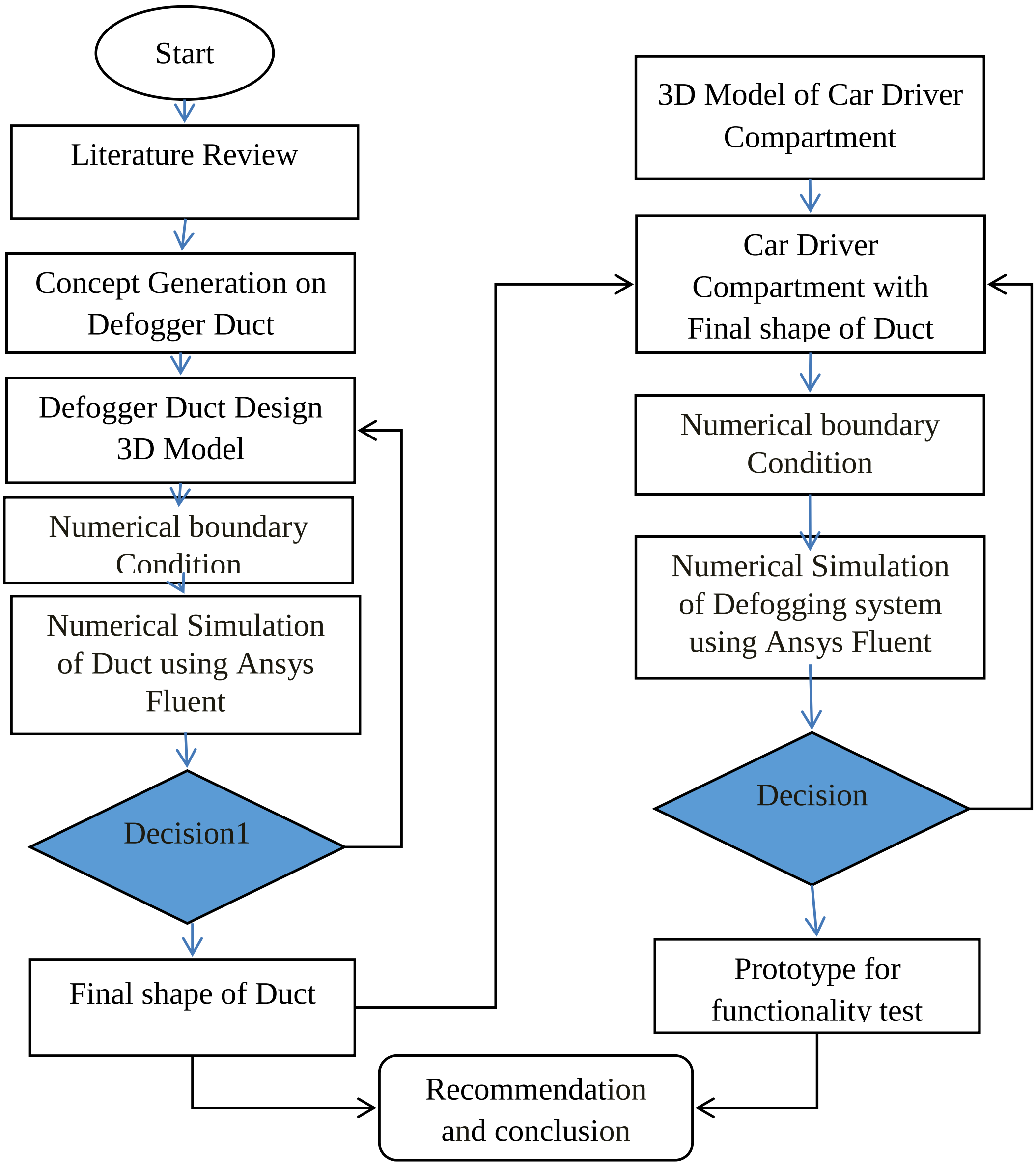

Figure 3.5. Methodology

3.4 Specific Literature Review for Defogger Design

It is known that data is the information gathered by a literature reviewer to inform a literature review. As a result, the literature review process can be considered as a data collection tool that is, a method of gathering a body of material pertinent to a certain topic of interest. Therefore the collected data for the analysis of defogger is based on primary and secondary type of Data.

3.4.1 Primary Data

It is known that a primary data source is an original data source, that is, one in which the data are collected firsthand by the researcher for a specific purpose. Primary data are usually collected from the source-where the data originally originates from and are regarded as the best kind of data in research. There for the researcher collected the following data as a primary, which has shown by Dimensions and 3D Model of Toyota HAICE 2004 Quarter part. The model of Toyota HAICE is shown figure 3.6.

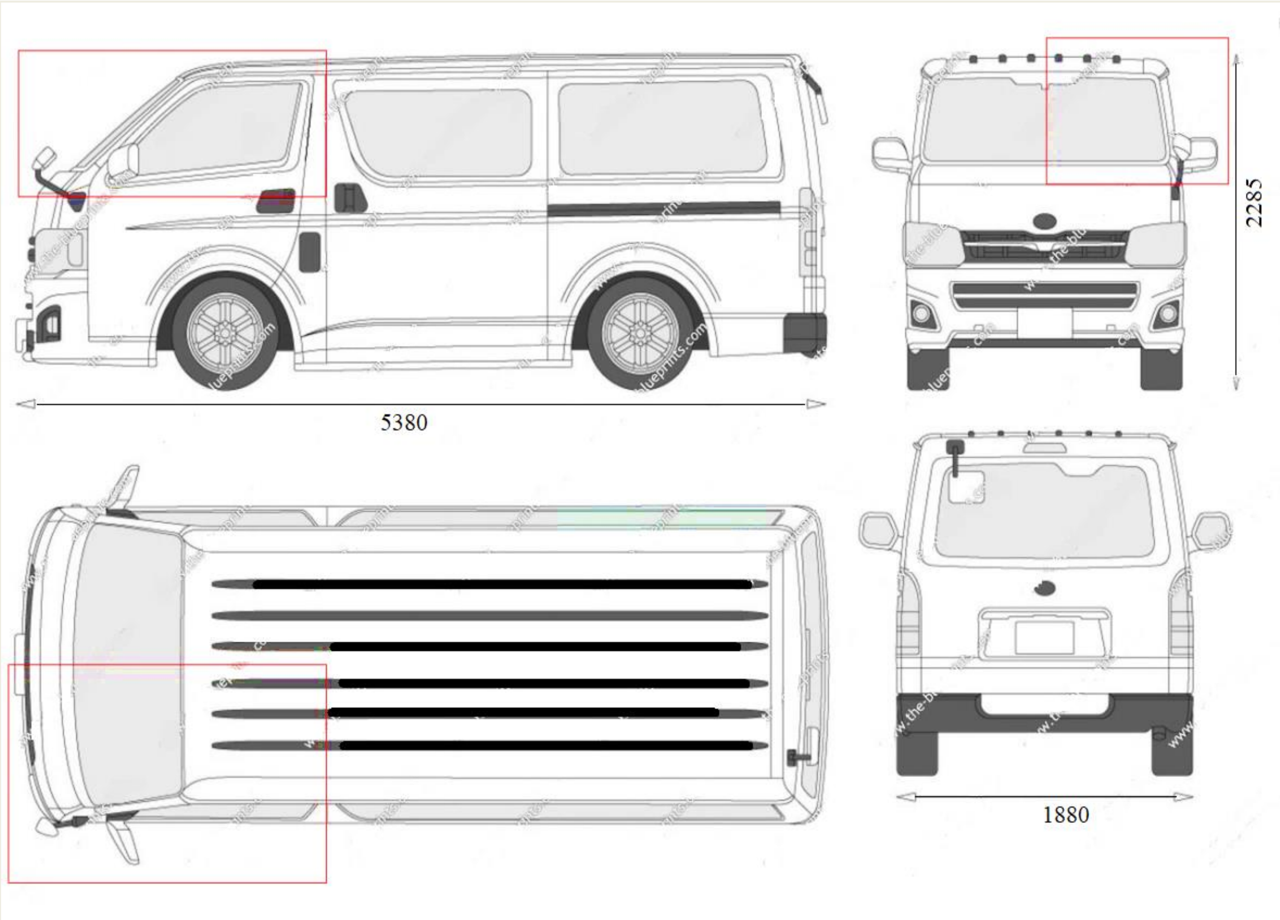

Figure 3.6.Toyota HAICE 2004 Car Dimensions (https://www.the-blueprints.com/toyota_hiace/)

Existing Defogger Machine

This car heater may be used as a cooling fan to provide breeze in the summer, as well as defrosting/demisting windows and windscreens. All that is required is to flip a switch, and the hot or cool air will be released as needed. This item is a vehicle-specific high-power electrical appliance with a rather high working current (about 12.5A). It will not be able to function for an extended period of time (40-60 minutes).Heats up quickly: The innovative design of the air outlet provides high-efficiency heating, removing frost, fog, and mist from the vehicle's windshield swiftly and safely, and ensuring driver safety. If the machine starts up for a few minutes during use, it will immediately stop. This is due to the present protector's inadequacy.

All 12V Vehicle Cars are compatible. This is a high-power electrical appliance; the plug should be inserted snugly when in use to maintain excellent electrification, and touching the cigarette end metal parts with hands may cause burns when the plug is pulled out after a long period of usage. Existing Defogger Machine is depicted in Figure 3.7.

Figure 3.7.Existing Defogger Machine

3.4.2 Secondary Data

Material Properties

To specify the conditions and material qualities independently, the numerical model is constructed with a specified control volume for the automotive inside, frost layer on the windshield, side glasses. Table 3.2 shows the material properties used in the numerical studies. The wind-shield and side panels were given car glass characteristics. To better understand the phase shift, the latent heat, solidification temperature, and liquefaction temperature of ice are shown.

Table 3.2.Material properties used in the analysis.

Material	Air	Car glasses	Frost Layer
ρ $[kg/m^3]$	1.206	2190	917
$\mu x 10^{-5}$ $[pa.s]$	1.83		0.00553
C_p $[J/kg.K]$	1007	740	2027
K $[w/m.K]$	0.0256	1.38	2.25
Latent heat [J/kg]	-	-	334.96
Solidus Temp [K]	-	-	271
Liquidus Tem [K]	-	-	274
Thickness (mm)	-	6	0.35 - 1

3.5 Concept Generation and 3D Model of Defogger Duct

It is known that a conceptual model is a perceptual representation of how something should be done that researcher have. Many times Conceptual modeling is done at an early stage in the design process to gain a fundamental understanding of how users think about activities, which can later be used to solve mathematically, like numerical analysis. On this research the concept generated for design is that of, can be used both windshield defogging and side window glasses. The conceptual 3D model of defogger is shown with figure 3.8. The concept has been generated by making the exit port very thin in order to maintain the inlet port and exit port flow speed with in the range of previously conducted standard testing of laboratory on defogging experiment. One the exit speed of flow is fitted with standard, the realistic simulation has been started by modifying the basic parameters on conceptual defogger, and these are rounding the bottom corner edge, modifying the exit zone by fin like multiple ports and adding flow deflector at some special location. Figure 3.8 shows the original 3d model of new concept.

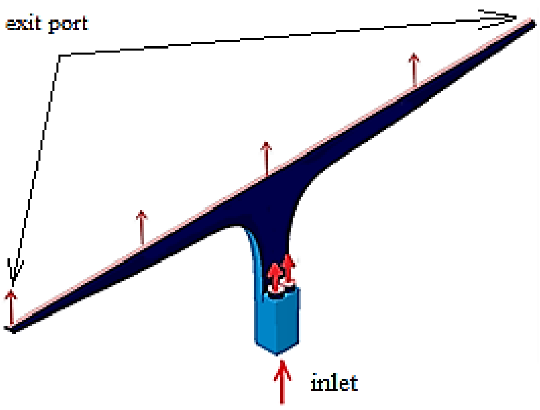

Figure 3.8. 3D model New Concept of Defogger Machine

Basic parameter

The basic parameter to test the numerical analysis of defogging is, eulerian film thickness considered as input and the output is defogging period whether it is long or short. In contrast to film thickness considered as a droplet, raindrops typically have sizes of the order of 1 mm, with observed maximum sizes in nature of around 5 mm in tropical rain. Raindrops in natural rain cannot reach arbitrarily large sizes. Heavy rain can be greater than 4mm per hour. Considering this phenomena the simulation has been performed at 5mm eulerian film tickness inorder to consider the worstcase scanerio. Droplet has been shown and displayed on following figure 3.9. The Simulation has been carried out by varying the tickess of fluid film from 0.35 mm, 0.75, 1.07 and 1.4mm. all results are recorded by checking deffoging period.

Figure 3.9Maximum size of droplet

3D Model of Toyota HAICE 2004 Driver's compartment

The driver's compartment is the space dedicated solely to the driver and contains the driver's seat, steering wheel, controls, instruments, and other driving-related gear. The driver visibility is special issue at this quarter area there for the research has been focused on this compartment area. The following figure shows the 3D model of quarter sector of car that consider only driver region. Figure 3.10 shows 3d model of driver compartment.

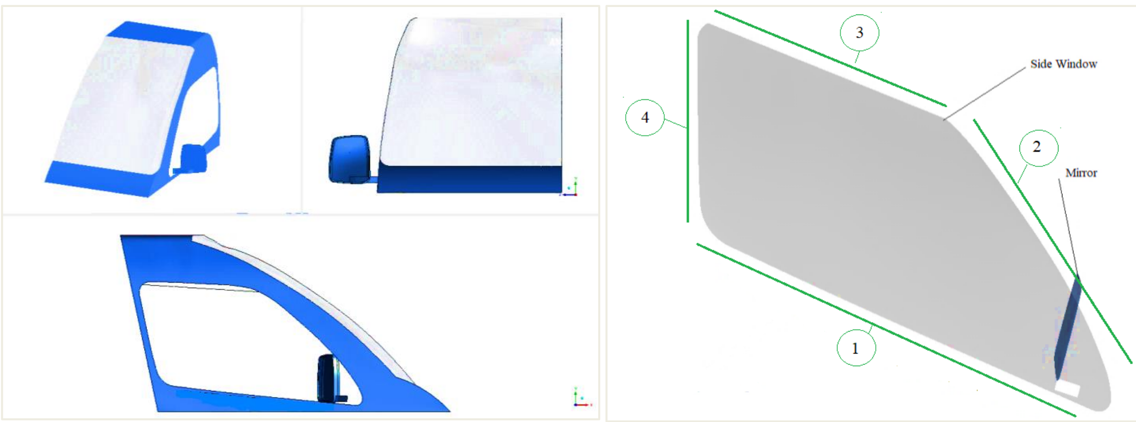

Figure 3.10. 3D model of Driver compartment

The number 1 - 4 on side window glass is representing alternative position of defogger machine. Out of these 4 alternative positions available, number (2) position is better for defogger base on its safety.

3.6 Numerical Boundary/Initial Conditions

The flow medium has been chosen as air, and its physical parameters have been chosen at ambient conditions. The temperature in the compartment and on the side window was initially -6°C. The defogger inlet port was used to inject air at a speed of 14 m/s with a 45-degree injection angle. The angle formed by the window glass and the incoming flow from the defogger duct is known as the injection angle (45 degree). Over the course of 30 minutes, the transient inlet temperature ranged from -6°C to 37°C as the initial and final temperatures, respectively. For the outflow condition, a fixed static pressure was used. Except for the side windows and windshield, the entire compartment was assumed to be adiabatic for the boundary condition. The ambient temperature was estimated to be around 6 degrees Celsius and isothermal. Cold room testing is used to determine window defogged patterns in accordance with FMVSS 103 regulations. Frost layers have been modeled as eulerian film with thicknesses of, 0.35 mm, 0.75, 1.07 and 1.4mm. The nozzle design's window defogged melting pattern is appropriate because it complies with FMVSS 103 criteria. All windows are depicted as closed unless otherwise specified.

3.6.1 Numerical Simulation Procedure

Computational Fluid Dynamics (CFD) is the analysis of fluid flows using numerical methods. Using CFD can analyze complex problems involving fluid-fluid, fluid-solid, or fluid-gas interaction. Therefore, if somebody wants to simulate flow behavior, the following term should be the first concepts can formulate the Flow Problem

- Model the Geometry and Flow Domain
- Establish the Boundary and Initial Conditions
- Generate the Grid
- Establish the Simulation Strategy
- Establish the Input Parameters and Files
- Perform the Simulation
- Monitor the Simulation for Completion

The general numerical technique that used on this research work is explained in detail by the sequential stepsin the following flow chart in figure 3.11.

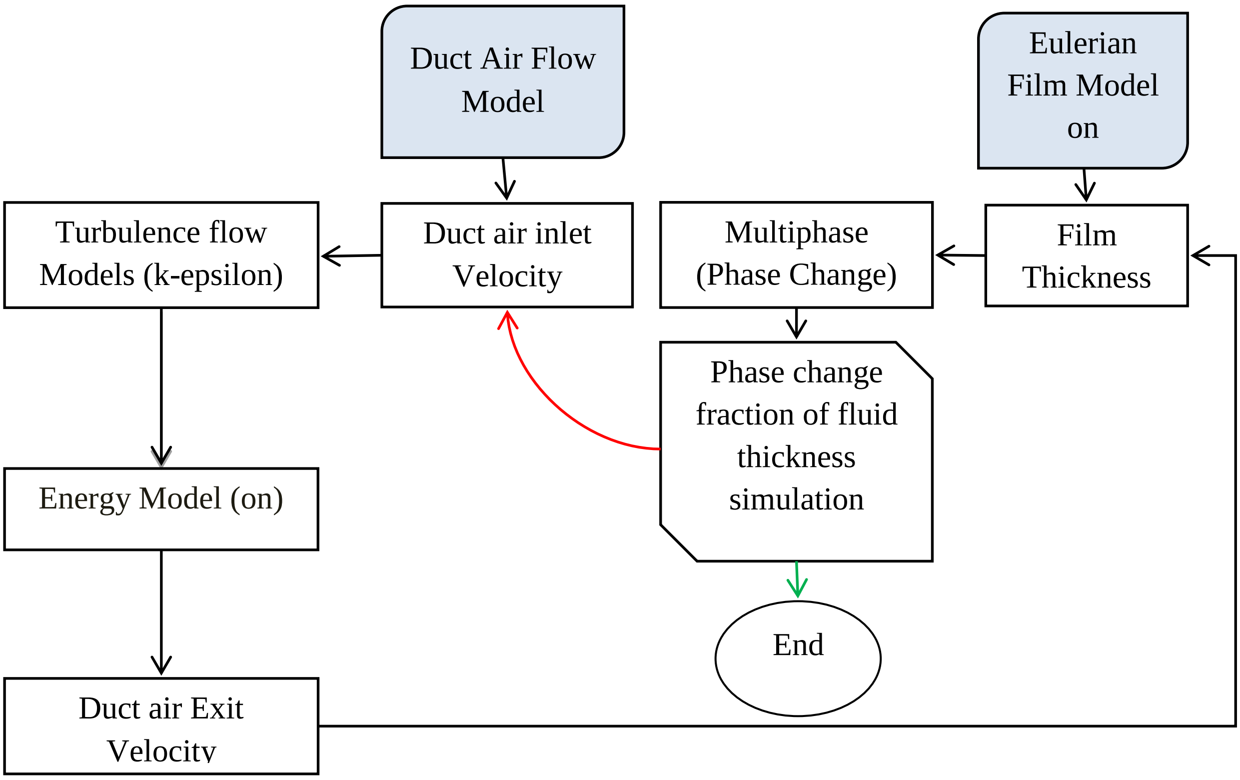

Figure 3.11.Steps involved in Numerical Method

3.6.2 Numerical Simulation of Unfreeze

Visibility through the car windshield is critical, especially in very cold temperatures when ice forms on the side window screen. Nonetheless, because phase shift is involved, numerical simulation of the unfreeze process is a difficult undertaking. A finite volume computational fluid dynamics (CFD) tool is used to calculate the numerical solution in this thesis. The temperature of the wind shield and driver side glass widow during a certain period, which causes frost to melt on the widow and the time it takes for the frost to melt, must meet the SAE J902 standard.

3.6.3 Governing Equation

Several engineering applications involve thin liquid film. In ANSYS Fluent, Eulerian Wall Film Model (EWFM) is developed to satisfy this need Peng KE, Jie LIU, Yi LU (2019). There are several different physical phenomena associated with a liquid film that must be modeled. For example in automotive applications, Defogging/demisting of the windshields, Oil filtration, and separators. Water film on the rearview mirror, Piston cooling, and Coating processes. Therefore the governing equations used to solve this type of numerical simulation are Peng KE, Jie LIU, Yi LU (2019).

Mass Equation

$$\frac{\partial \rho u_i}{\partial x_i} = 0 \tag{1}$$

Momentum Equation

$$\frac{\partial \rho u_i}{\partial t} + \frac{\partial u_j \rho u_i}{\partial x_j} = -\frac{\partial p}{\partial x_i} + \frac{\partial}{\partial x_j}\mu\left(\frac{\partial u_i}{\partial x_j} + \frac{\partial u_j}{\partial x_i}\right) - \rho g_i \beta (T - T_o) \tag{2}$$

$$Where\ \mu = \mu_1 + \mu_2$$

$$\mu_1 = Laminar\ Coefficiet\ of\ Viscosity$$

$$\mu_2 = \frac{C_t \rho k^2}{\varepsilon} = Turbulent\ Coefficiet\ of\ Viscosity$$

Energy Equation

$$\frac{\partial \rho c_p T}{\partial t} + \frac{\partial u_j \rho c_p T}{\partial x_j} = \frac{\partial}{\partial x_i} K\left(\frac{\partial T}{\partial x_i}\right) + \dot{q} \tag{3}$$

The turbulence was modeled by standard k-ε equation:

$$\frac{\partial \rho u_i}{\partial t} + \frac{\partial u_j \rho u_i}{\partial x_j} = -\frac{\partial p}{\partial x_i} + \frac{\partial}{\partial x_j}\mu\left(\frac{\partial u_i}{\partial x_j} + \frac{\partial u_j}{\partial x_i}\right) - \rho g_i \beta (T - T_o) \tag{4}$$

$$\frac{\partial \rho k}{\partial t} + \frac{\partial u_j \rho k}{\partial x_j} = \frac{\partial}{\partial x_j}\left(\frac{\mu_t}{\sigma_k}\frac{\partial k}{\partial x_j}\right) + G_s + G_T - \rho\varepsilon \tag{5}$$

$$\frac{\partial \rho \varepsilon}{\partial t} + \frac{\partial u_j \rho \varepsilon}{\partial x_j} = \frac{\partial}{\partial x_j}\left(\frac{\mu_t}{\sigma_k}\frac{\partial \varepsilon}{\partial x_j}\right) + C_1 \frac{\varepsilon}{k}(G_s + G_T)(1 + C_3 R_f) - C_2 \frac{\rho \varepsilon^2}{k} \tag{6}$$

Where,$G_s = \mu_t \left(\frac{\partial u_i}{\partial x_j} + \frac{\partial u_j}{\partial x_i}\right)\frac{\partial u_i}{\partial x_j} G_T = g\beta\left(\frac{\mu_t}{\sigma_t} + \frac{\partial T}{\partial x_i}\right) R_f = -\frac{G_T}{G_s + G_T}$(7)

These equations include many empirical constants that are described as

$$\sigma_k = 1, \sigma_\varepsilon = 1.3, \sigma_t = 0.9, C_t = 0.09$$

$$C_1 = 1.44\ , C_2 = 1.92, C_3 = 1.3$$

The symbols used in the equations represent their usual meanings

Where,

$\rho\ is\ density\ of\ fluid, T\ is\ fluid\ temprature$,

$\varepsilon\ is\ epsilon\ which\ is\ energy\ dissipation, \mu\ is\ fluid\ vicosity$ and

$u_j\ fluid\ flows\ speed$

3.6.4 Defogger nozzle design

The defogger nozzle is part of the heater subsystem. Its primary function is to produce a jet flow in the direction of the window inner surface using a portion of the HVAC unit flow directed from the general assembly into the nozzle inlet. The heated air passes through the nozzle configuration and exits. The hot jet leaving from the defogger nozzle warms up the glass' inner surface, thus, melting any frost/ice layer that may store on its outer surface. The defogger nozzle also helps as purpose to circulate the air in the neighborhood of the glass to prevent fogging when the glass' inner surface temperature becomes lower than the dew point temperature of the compartment air. The performance of the defogger subsystem is normally evaluated by its capability to quickly remove frost/ ice and its ability in preventing the windows from frosting over again. Several factors came into play to demonstrate the interaction of airflow with the glass widow inner surface and related design considerations required to provide a pure vision region. Proper placement, direction, and shape of the jet flow of the defogger nozzle are key rudiments in successful window clearing. To achieve the standards of operative performance, the defogger nozzle must be proficient in making airflow that scatters over the whole inner surface of the side windows with minimum offsetting of velocity and without any significant separation from the glass; the flow must have enough momentum to continue to be attached as it approaches the upper edge of the window. Defogger performance standards specify that certain zones of the window must be cleared of all frost, ice, or snow accumulation within specified time frames; see the Table below, for it is based on the society of Automotive Engineering in Japan (SAE-J) and according to the federal motor safety standards (FMSS 103). The standards assume a full defog mode of operation at maximum blower speed to support FMVSS 103 requirements.Table 3.3 shows summery of standard defogger performance testing.

Table 3.3 Summary of defogger performance Standard

Area	FMVSS 103	SAE J902
“C” Driver Side	80% in 20 min	100% in 30 min
“C” Passenger Side	80% in 25 min	
A (vision area)	95% in 40 min	80% in 30 min

The average uniform velocity U at the exit of the nozzle is to be 6 m/s based on the measured standard flow for passenger car defogger design. Defining the hydraulic diameter at the defogger nozzle exit cross section. The Reynolds number of the flow, based on D_H, is calculated to be

$$\mathrm{D_H} = \frac{\mathrm{4Area}}{\mathrm{Perimetr}} \tag{8}$$

The Reynolds number of the flow, based on DH, is calculated as,

$$\mathrm{R}_{eH} = \frac{UD_H}{v} = 1.2x10^4 \tag{9}$$

Where μ is the kinematic viscosity at a temperature of 300 K and atmospheric pressure. This value for the Reynolds number suggests that the defogger flow is indeed turbulent. This determination is essential in establishing the characteristics of the CFD model. There for the model equation selected for different defogger nozzle duct design has been k epsilon model. From the above figure, blue line color represents the orientation of inlet hot air for windshield and side glass defogger.

3.6.5 Grid Independence Test

Several CFD research used grid independence tests to determine the best grid number. Based on the evaluation of various grid conditions, the grid independence test is a procedure for determining the ideal grid condition with the fewest number of grids without causing a difference in numerical results. The following table 3.4 is the result error % of grid test for both model of defogger and quarter car model. The error is determined by change in numerical result between better size grid (small size) and first grid size grid element. It is described that average velocity is for defogger and volume fraction for specified time step is numerical result for grid test of quarter car model.

Table 3.4.Grid Independence Test

Defogger, Tetrahedral meshes			**Quarter Car Model ,** (polyhedral)		
Element Size (mm)	Exit air Velocity (average)	Error %	Element Size (mm)	Film Volume fraction	Error %
11	1.78	53%	18	0.876	
9	2.74		15	0.745	15%
7	4.16	51%	12	0.652	12.5%
5	5.62	35%	9	0.613	5.98%
3	5.84	4.0%	6	0.582	5%
1	5.99	2.6%	3	0.5738	1.4%

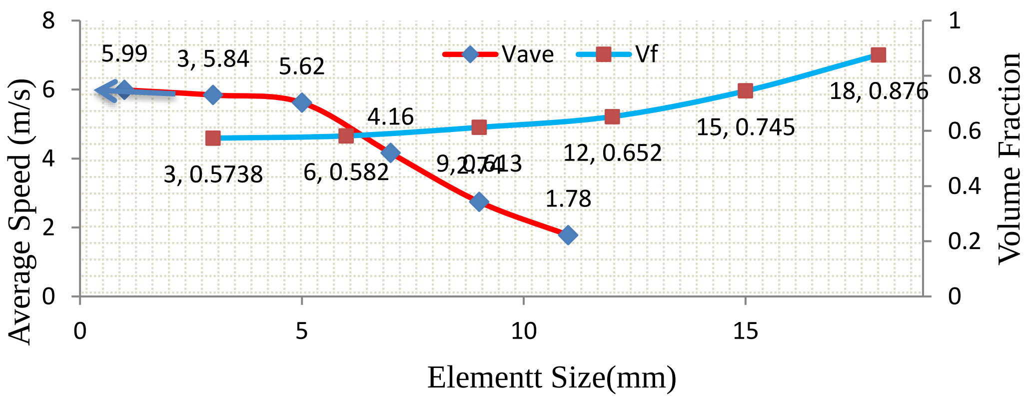

Figure 3.12.Plote of Grid Independence Test

The above table 3.4 and figure 3.12 of grid test shows that the minimum error of velocity is occurs between 3 and 1mm element sizes for defogger and between 6 mm and 3 mm sizes is minimum error on car quarter model. Therefore, considering also computational time cost. The selected element sizes are 2mm and 5.5mm for defogger and quarter car model respectively.

3.6.6 Selected Discretization Size (mesh)

Discretization is the method through which transform continuous variables, models, or functions into a discrete form. This is by making a set of contiguous intervals (or bins) that go across the range of our desired variable/model/function. Continuous data is measured, while discrete data is counted. Therefor the discretized three different model of defogger duct and Haice 2004 Quarter model are shown as figures 3.13& 3.14 respectively.

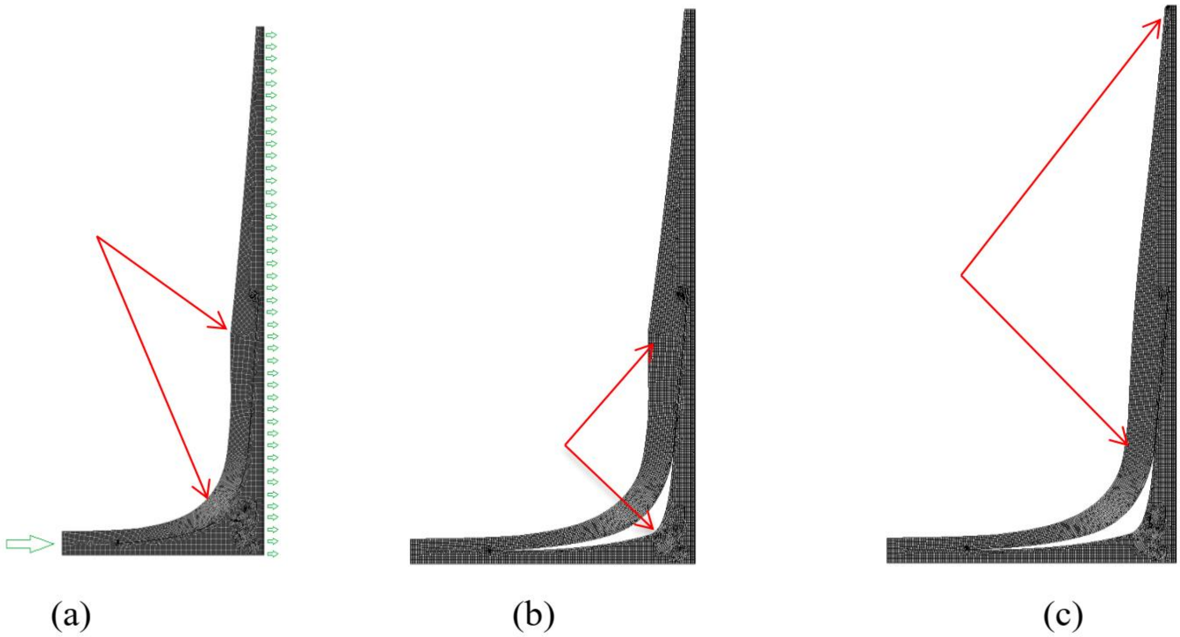

Figure 3.13. Discretized model of Symmetry Design of three concepts Defogger Duct

The three figures are different based on highlighted modification of defogger duct wall.Figure (a) has fileted corner and has small gone. Also it has this defogger wall when it compared with figure (b) & (c). Figure (b) has cut at the middle of fluid flow and it has large gone than figure (a) & (c). Finally figure (c) is verily flatter than both remained figure with its middle cut.

Model Quarter Car Polyhedral mesh

The main benefit of polyhedral mesh is that each individual cell has many neighbors, so gradients can be well approximated. Polyhedrons are also less sensitive to stretching than tetrahedrons which results in better mesh quality leading to improved numerical stability of the model. There for the mesh used on this numerical simulation is polyhedral mesh.

Mesh Generated of Model Quarter Car

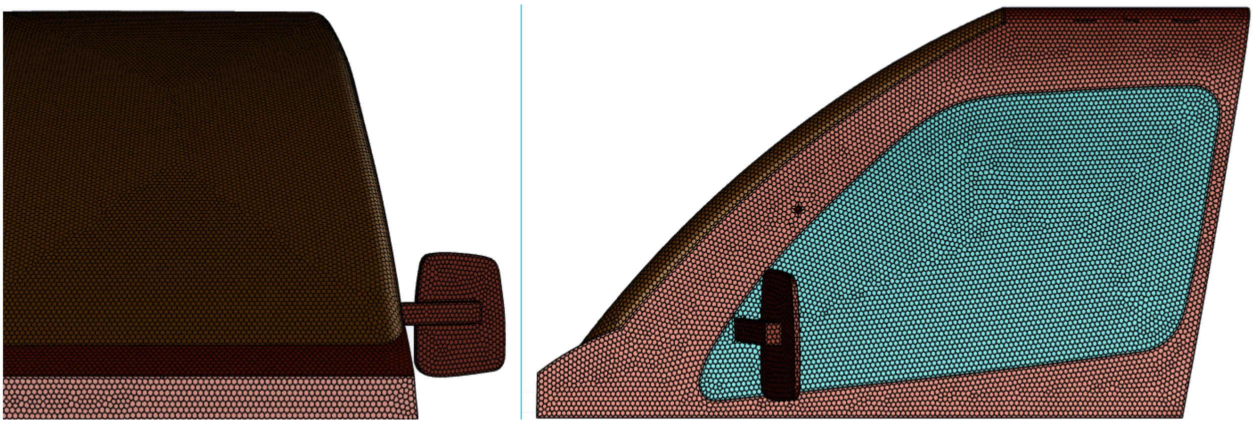

Figure 3.14.Mesh (polyhedral) Generated of Model Quarter Car

Quarter car Model for simulation

The following figure 3.15 is imported to the fluent solver for defogging case

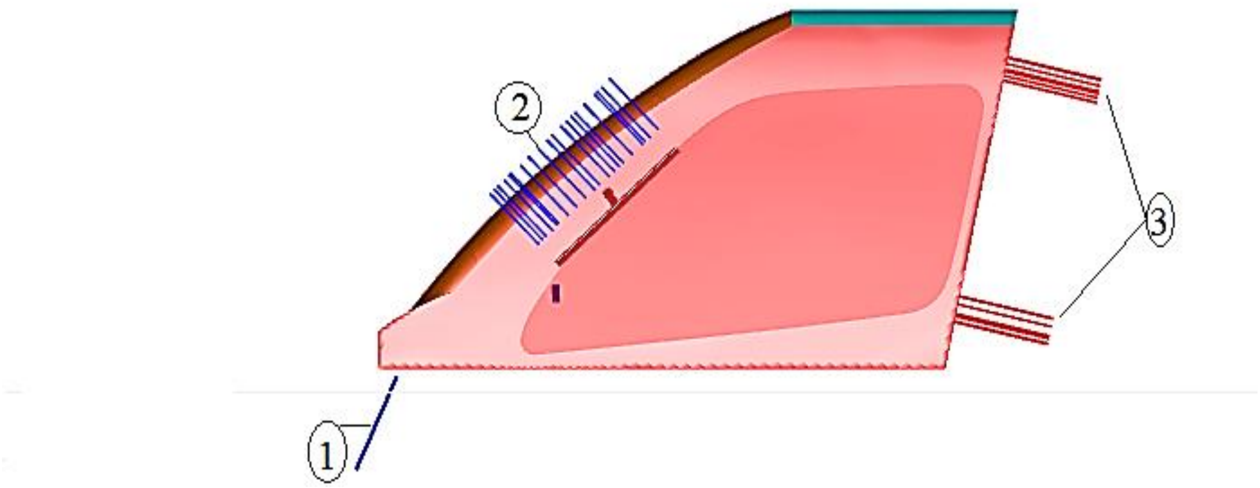

Figure 3.15.Orientation of Defogger inlets

From figure 3.15, (1) represent the input hot air region to the windshield, (2) input hot air region to the side window glass and (3) pressure outlet on boundary zone.

CHAPTER FOUR
RESULTS AND DISCUSSIONS

4.1 Defogger Duct Velocity and pressure Contour

The defogger performance simulation is performed in four steps based on different shape of nozzle bottom fillet diametric size 45, 55, 65mm and cut blue color contour zone. The defogging simulation is performed by steady state solution. The objective is to select better shape velocity and pressure distribution. The velocity distribution at the outlet is also recommended to be included as a design value, because at the exit of defogging duct the velocity of the nozzle must meet with the standard of maximum 6 m/s. The following figures 4.1 are show the flow distribution contour profile of velocity and pressure. From the figurepressures and velocity, distribution of the fourth or cut blue color contour zone is highly acceptable when it is compared with others. It has equal flow distribution at the exit zone. However, the flow at the exit of ductcannot reach evenly all surface of the window for the defoggerexit zone has paired open and closed port which is 8 ports closed and 7port opened.

A) Rounding the corner

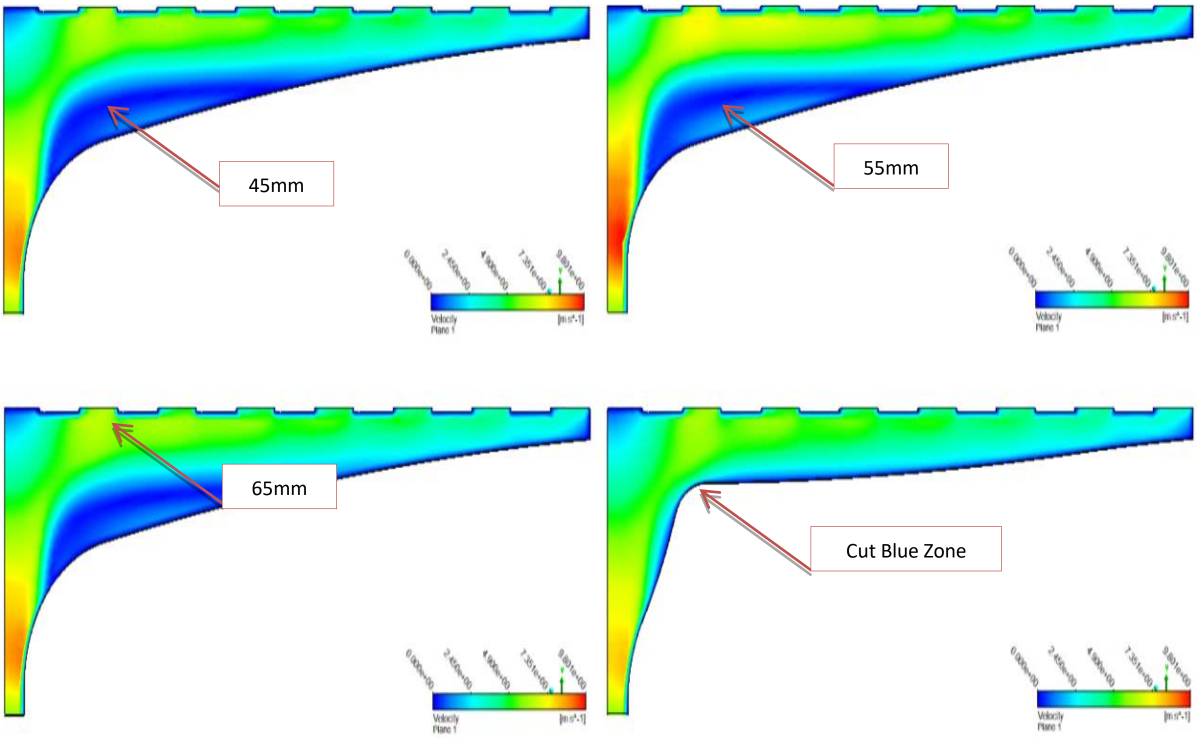

(a)

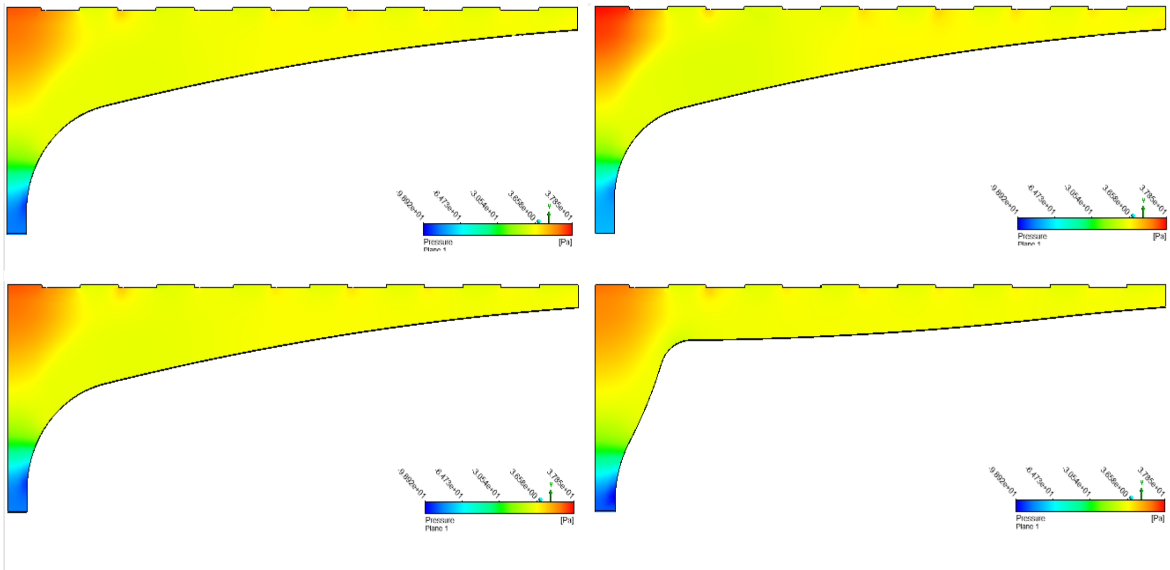

(b)

Figure 4.1. (a)Velocity distribution, (b) pressure contour

B) Orientation of deflector’s

In order to overcome the problem of the duct flow not reaching evenly, all surface of the window for the defogger exit zone that has paired open and closed ports, which is 8 ports closed and 7 ports opened. The researcher has decided to open all ports merged into one exit zone. The deflector is used as flow separation to minimize the flow focused on straight out. In addition, deflecting the flow pattern on the exit zone effectively. The optimum shape of the duct is concluded with these three deflector features founded on the defogger shape. Finally, the blue zone should be removed physically to minimize geometry size or weight also. The following figure, 4:2-4:3 shows the modified defogger's final shape.

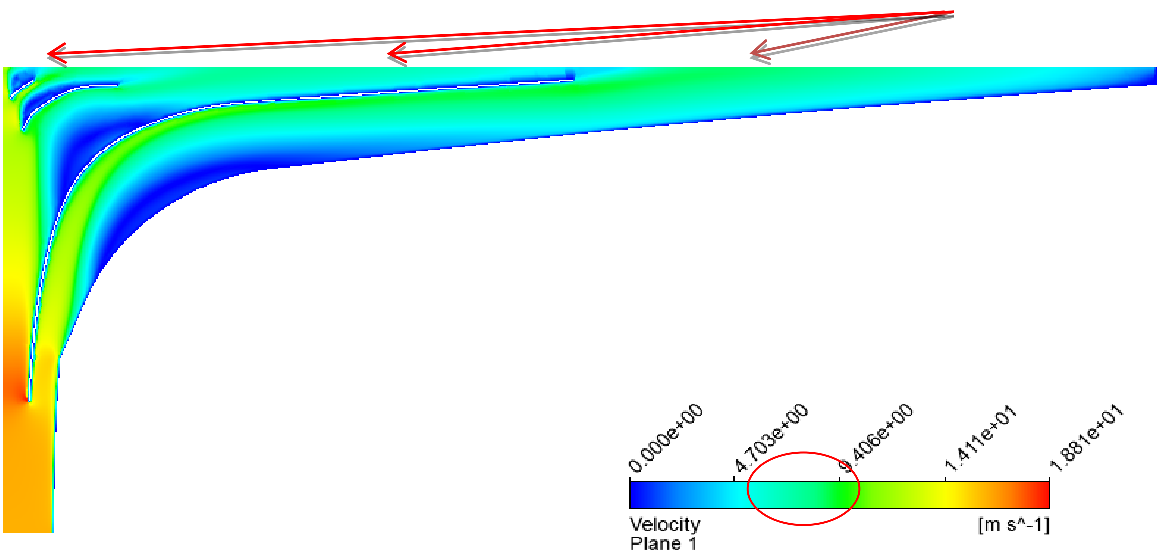

(c)

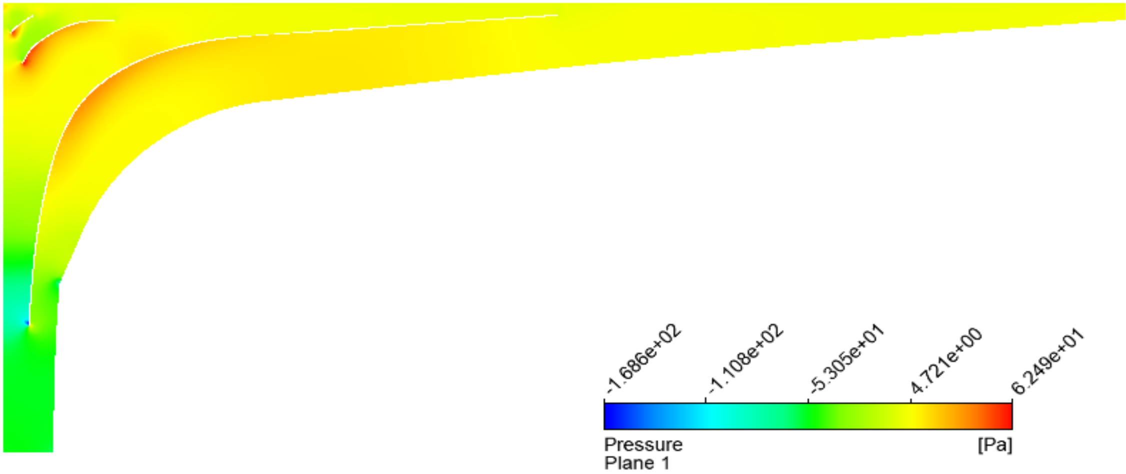

(d)

Figure 4.2.(c) Velocity distribution, (d) pressure contour

C) Deflector's orientation and cut blue zones

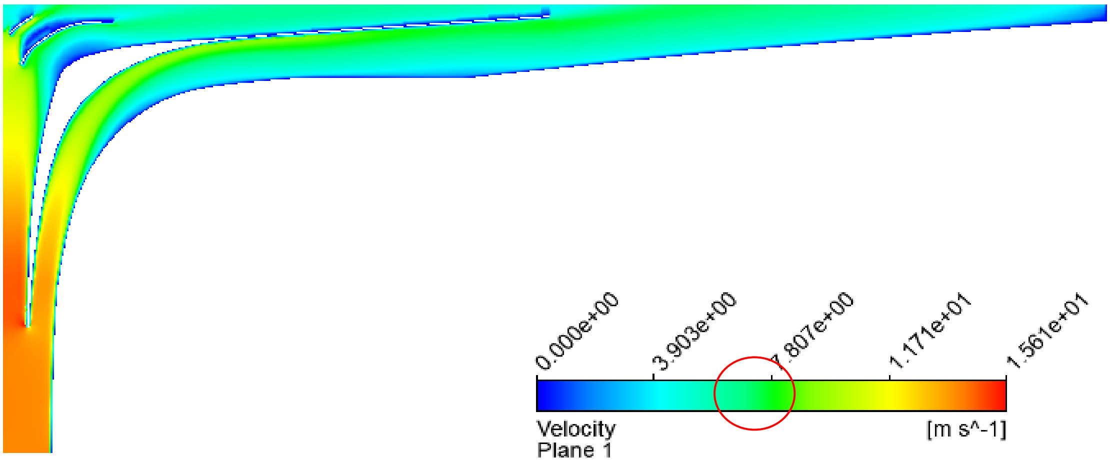

(e)

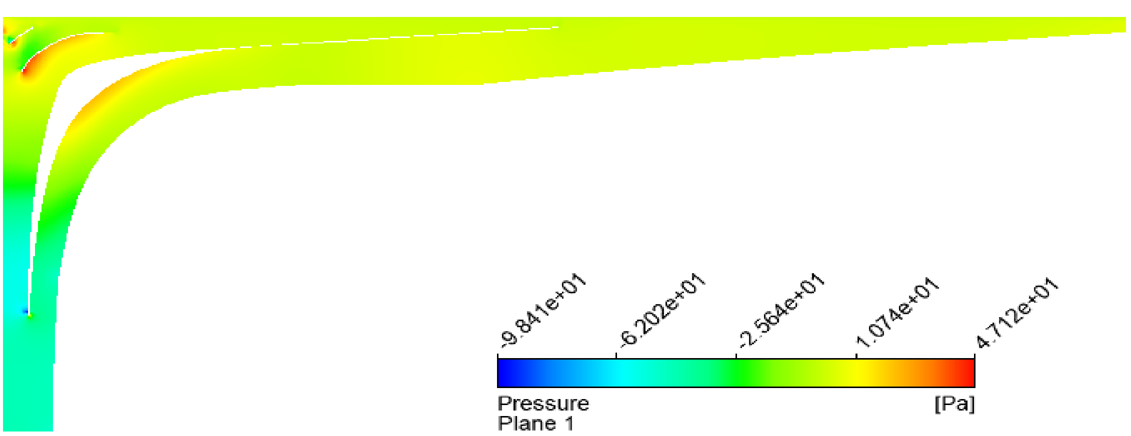

(f)

Figure 4.3. (e) Velocity distribution, (f) pressure contour

D) Deflector's orientation and cut blue zones with filleting

Removing the cornering edge features from the modified form of defogger options is used to increase the performance of the machine. By fileting the edge, the flow behavior of hot air or cold air can reach immediately exit port without excessive loss. The following figure 4.4 shows the removed edge form of the final shape of the defogger wall.

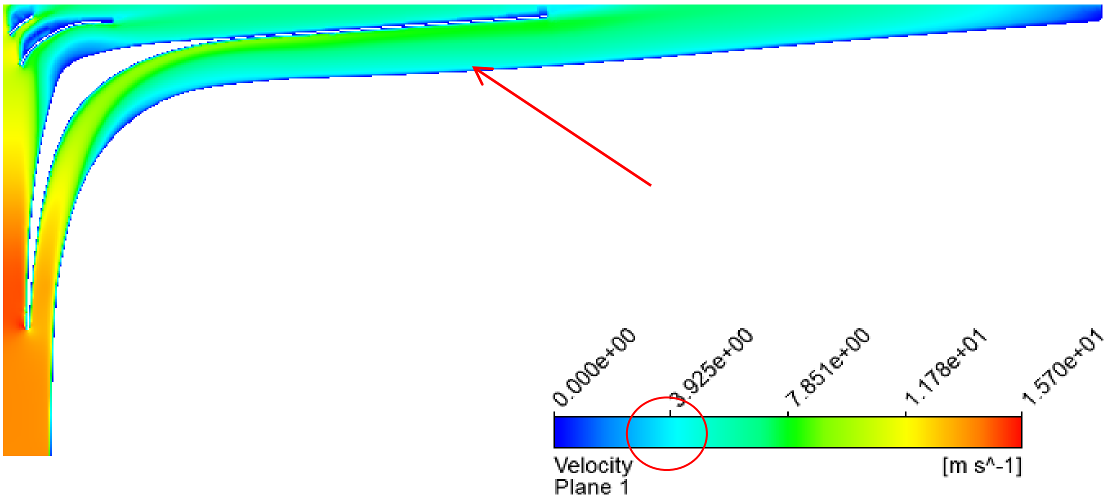

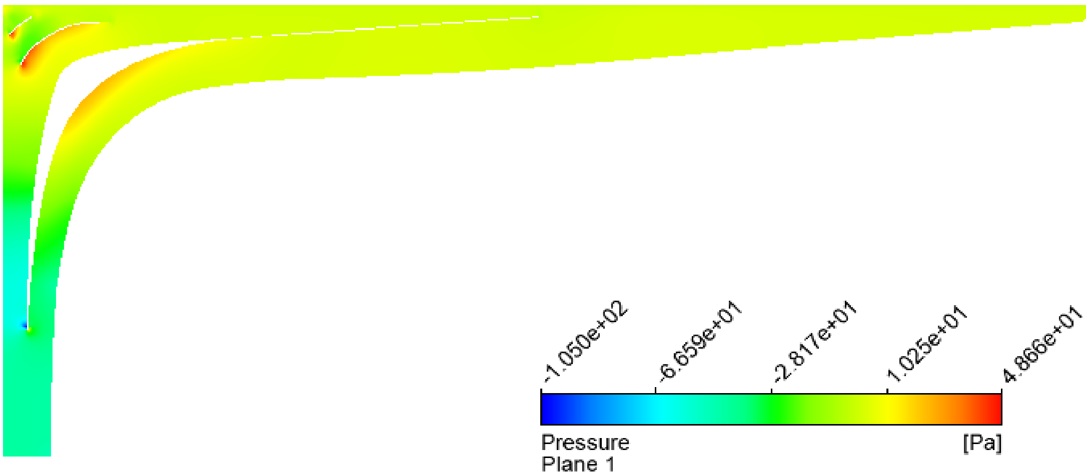

(h)

Figure 4.4.(g) Velocity distribution (h) pressure contour

4.2 Optimized shape ofDefogger wall

The 3d model of optimized shape of defogger wall is shown in figure 4.5

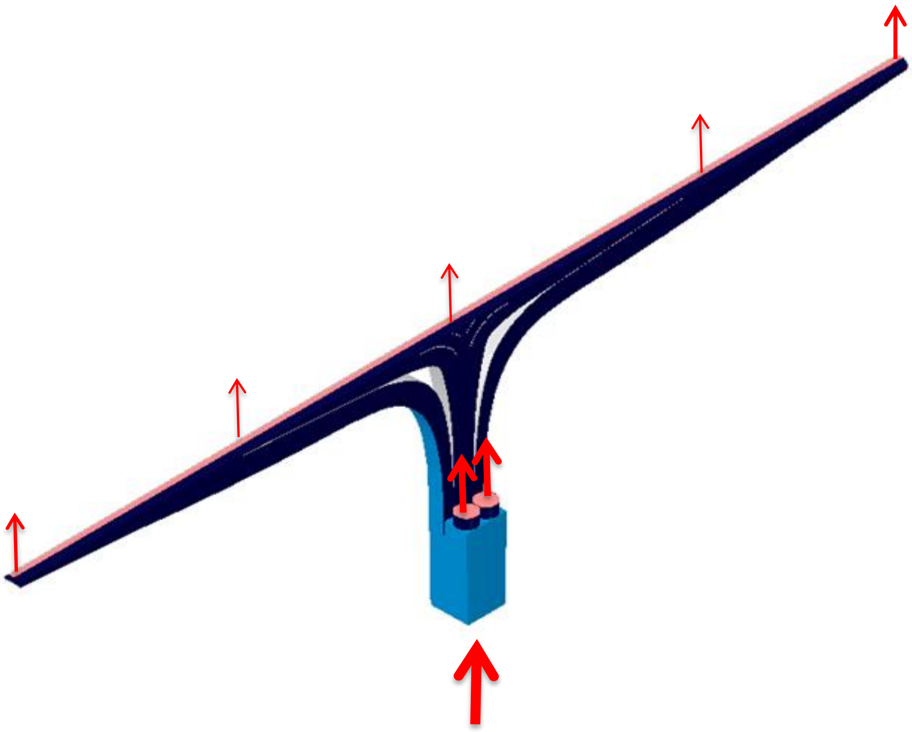

Figure 4.5.Defogger Machine for Manufacturing

Based on the simulation of different modified features on defogger wall, the final object of defogger is contained by one import and three exit port for three widows, which are two side glass ad one windshield.

The flow Exit port of defogger wall is very thin, because it is tuned until the design point speed reached which is standard of FMVSS or SAE not more than 6m/s for hot air blowing to the glass. But input is air flow speed of 14m/s.

4.3 Simulation of Defogging on Quarter car

Contour plot of film thickness defogging simulation results are described by two orientations. This contour plot is this of 5mm film thickness that has been considered as worst cases, because it can be considered as maximum fluid film thickness of fog. The next is the graphical plot of film thickness variation to examine defogging period. Variable film thickness 1.4mm, 1.05mm, 0.7mm, and 0.35mm are simulated and descried by fitted smooth curve.

A) Orientation (1)

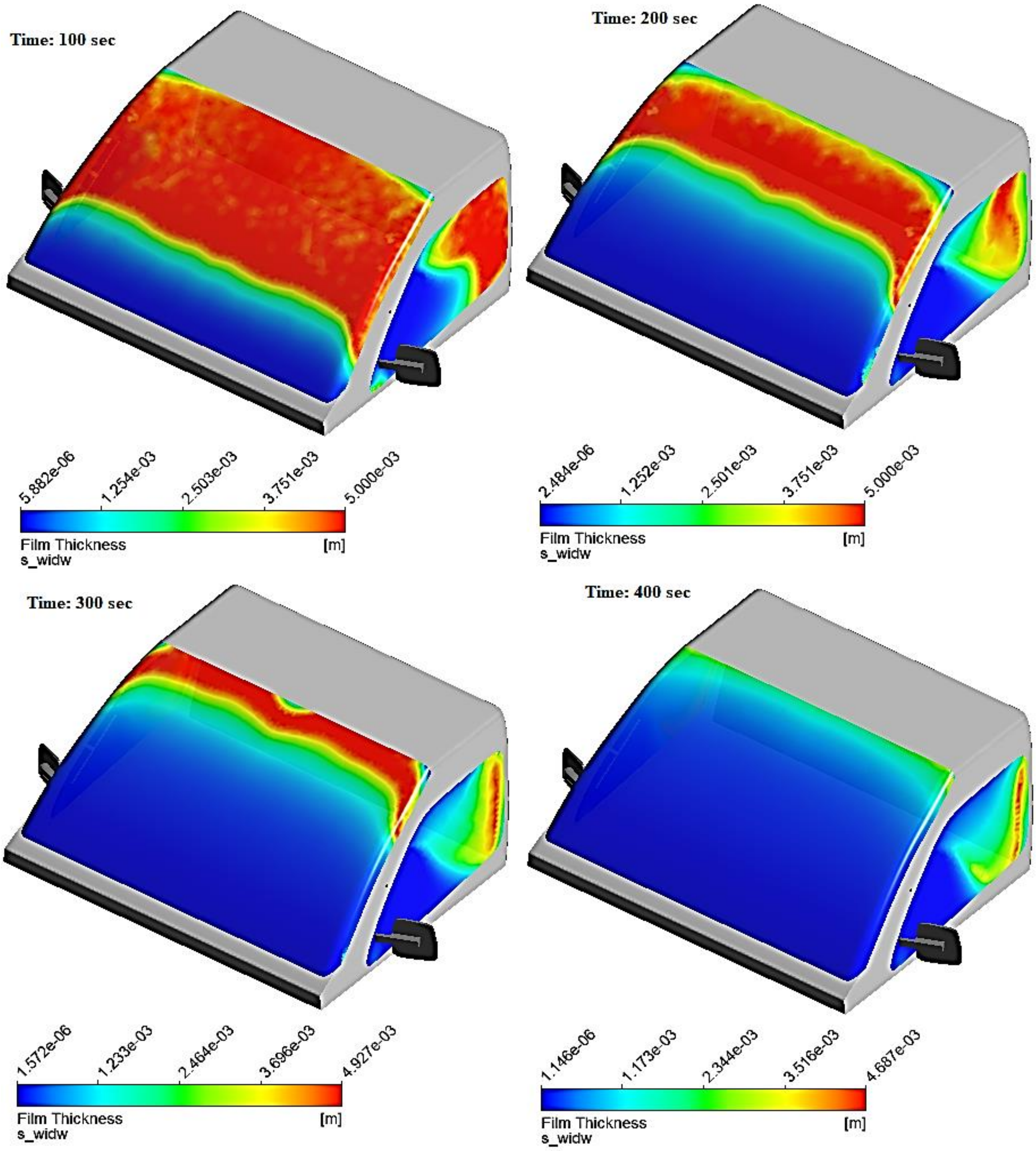

(a)

B) Orientation (2)

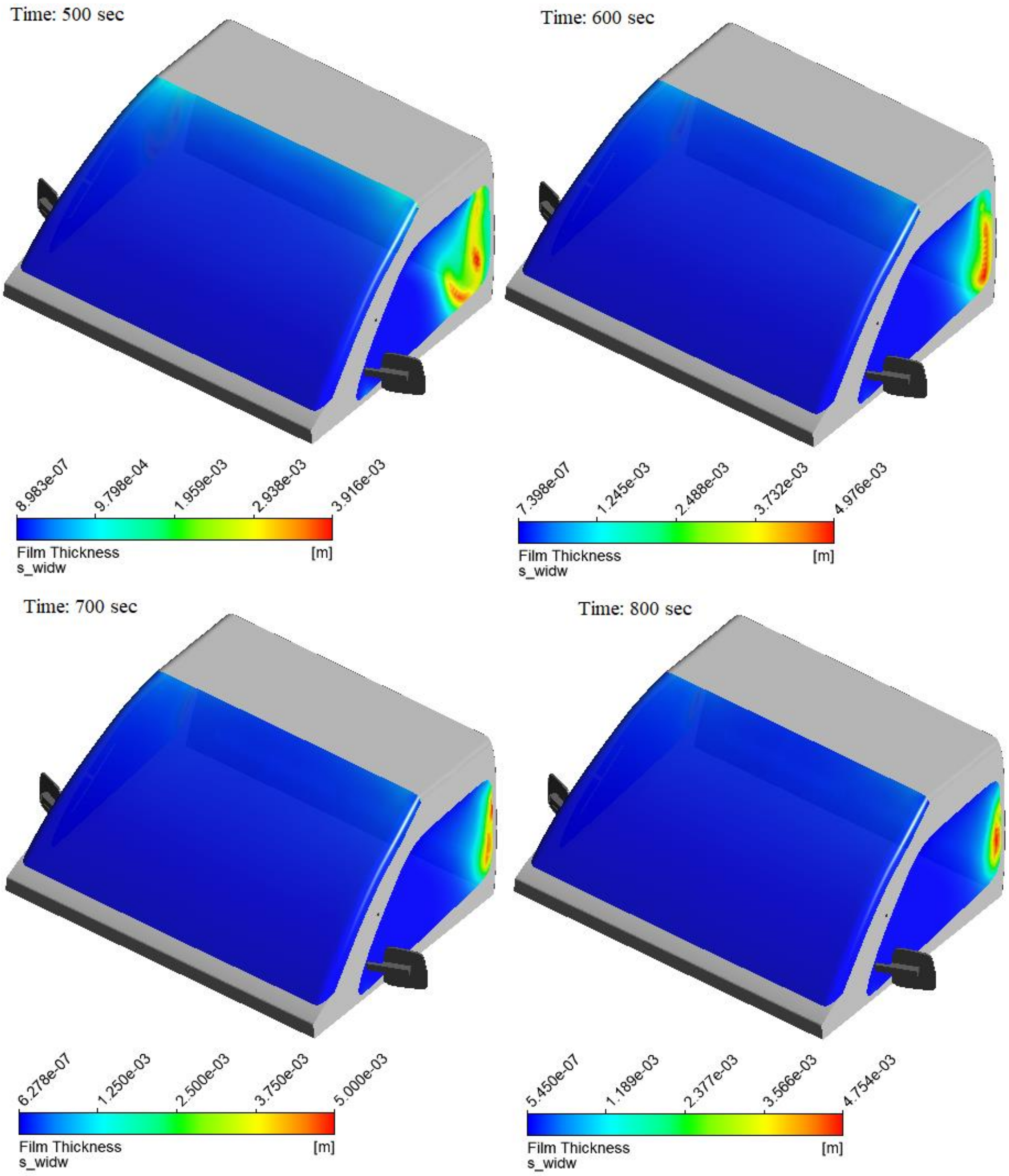

(b)

Figure 4.6. (a), orientation (1), (b) orientation (2) defogging Simulation of

4.4 Discussion

In this analysis of figure (4.6-4.7), CFD is used to simulate vehicle defogger, windshield and side glass flow and heat transfer to determine the velocity field and contours of defogged pattern in terms of the liquid fraction of frost. FLUENT with a defogging model based on the input temperature method is used in the simulation. The results provided an insight into the characteristics of the flow and defogger performance. Based on the melting pattern and time, it is observed that the performance of the current duct design meets the FMVSS 103 requirements.

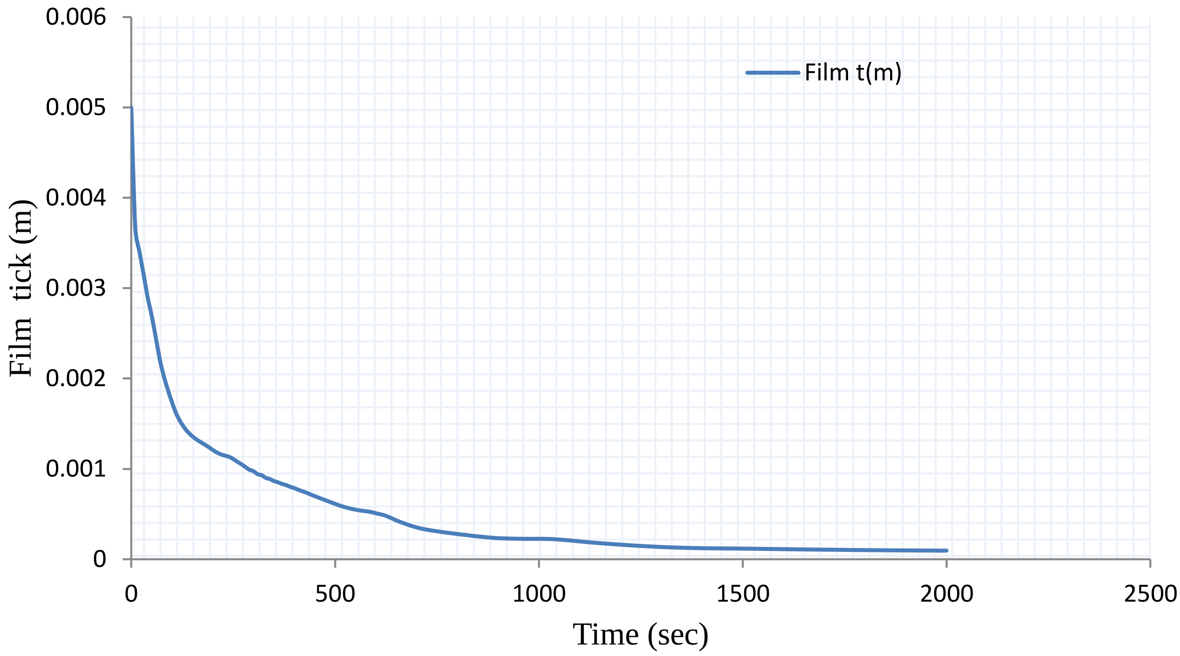

Figure 4.7.plot of full time Simulation of Defogging with time variant of drying glasses

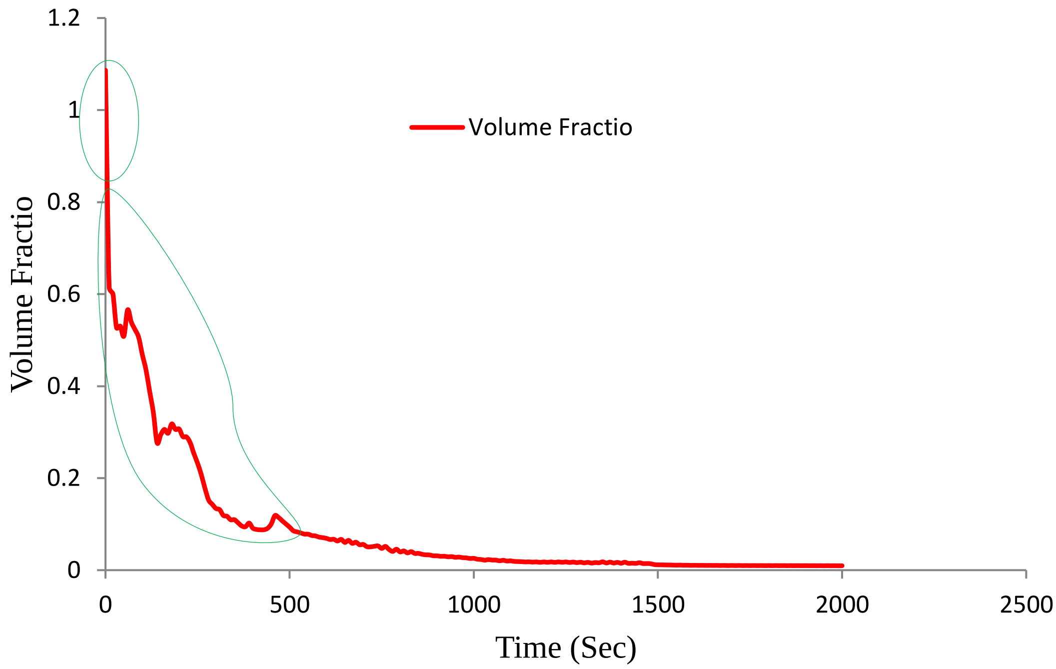

Figure 4.8.Fog melted Volume with respect to Time

From the above figure 4.8, melting is almost zero for up to 20 sec, and then frost starts melting at higher rate up to 500 second. The recommendation of the national highway traffic safety administration is that vision area A melted more than 80% and area C melted 100%, both within 2000 seconds (Kader et al, 2009). This analysis satisfies also society of automotive engineering (SAE) standard.

4.4.1 Frost volume fraction at different Eulerian film height

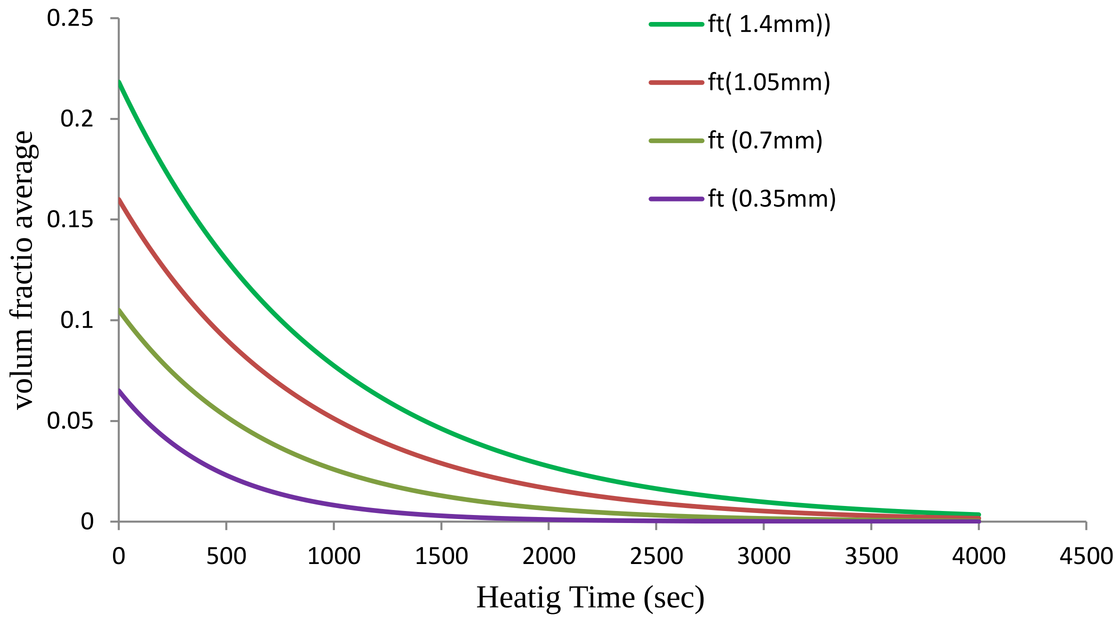

Figure 4.9.Frost melted Volume fraction with varied thickness

The liquid film thickness is applied to the window glass according to the experimental results from previous work of average non-movable liquid water film of 315.4 μm and 337.2 μm based on diode laser absorption spectroscopy (DLAS) and Ultrasonic pulse-echo method (UPEM) measurement recorded respectively. The hot air velocity is injected from the exit portion of the duct to the film surfaces on the glass windows. In order to investigate the effect of film wall thickness on defogging time, the film thicknesses of 1.4mm, 1.05mm, 0.7mm, and 0.35mm are simulated. The special parameter predicted here is the volume fraction of the water film that varied after a certain flow time. For all four different film thicknesses, the defogging performance simulation takes a time of 1500, 2500, 3000, and 3500 seconds, respectively, to remove all condensed water from the surface. Finally, the best option for this research work to design ShowTime defogging that no longer stays the ice on the surface. Therefore, the selected film thickness for high portables for three windows is considered as 1500-second taken film, which is 0.35mm.

CHAPTER FIVE
PROTOTYPING

5.1 Defogger Elements and Power EstimationFan

Electric fans have a motor that moves blades that are attached to a central rotating hub. Fans circulate air to cool and ventilate rooms and to control humidity. The work done by the fan is on air is calculated as,

AHP– Air Horsepower is work done by the fan expressed as horsepower.

$$\mathrm{AHP} = \frac{\mathrm{CFM}x\mathrm{TP}}{6356} \tag{10}$$

$$\mathrm{TP} = \mathrm{SP} + \mathrm{VP} \tag{11}$$

Where –TP Total Pressure,

-SP Static pressure

-VP- velocity pressure at any given point in a ventilating system.

- CFM. – Cubic Feet per Minute, is the volume of air moved per minute.

$$\mathrm{VP} = \left(\frac{\mathrm{FPM}}{4005}\right)^2 \tag{12}$$

Where, FPM. – Feet Per Minute, is the velocity of the airstream Air Horsepower become

$$\mathrm{AHP} = \frac{\mathrm{CFMx}(\mathrm{SP} + \left(\frac{\mathrm{FPM}}{4005}\right)^2)}{6356} \tag{13}$$

Air heater

Every air heater is comprised of two main components: - the first is a source of airflow. The source of air can be a fan, blower, or air compressor. The best source depends on the application and the type of heater. For example, a space heater does not need high velocity or specifically focused air, so a fan is used. In a more industrial application where a great deal of heat must be transferred in a focused stream, an industrial blower or compressed air is usually used.

A heating element

- For simplicity and portability, the scope of this work is limited to electric heaters. This type of heater has an element that is normally a coil of wire with a high resistivity. By passing an electrical current through the wire, heat is produced. The configuration of the resistance wire is dependent on the purpose of the heater. The element should not be powered without air flow, or it may overheat and burn out.

5.2 Heater Considerations

- Temperatures required in the process

  Every heater has a maximum rated operating temperature; however, this temperature is not attainable at all flow rates. Be sure that your heater has enough power (kW) to reach the target operating temperature at your desired flow rate. A heater supplier should be able to provide you with a flow versus temperature chart for a heater which will help to determine which model is right for the application.

- Size, shape and composition of objects to be heated

  The type and amount of material to be heated, the start temperature and final temperature required, and the heating time available must all be considered to determine how much power a heater must have for an application.

- Environment, losses, and inefficiencies

  The surrounding environment must also be taken into consideration when designing a system. For example, the volume of air in a chamber, any losses to the surrounding environment, as well as the material of a chamber walls must be compensated for with extra watts.

- Available voltage and amps

  Practical constraints can also limit the size of heater. Limited amperage or voltage availability can cap the watts for heaters.

5.3 Heating Element Power

To calculate the heat energy requirements for heating air or gases, the first step is to determine the flow rate in pounds per hour. If the density of the air or gas under the actual pressure is known, the kW requirements can be calculated directly.

$$L = Q / (c_p \times \rho \times (t_h - t_r)) \tag{14}$$

Where

L = *air flow rate* (m^3/s)

Q = *heat loss covered by the air heating system (kW)*

c_p = *specific heat air*

ρ = *density of air*

t_h = *heating air temperature* (^oC)

t_r =*initial wall or room temperature* (^oC)

5.4 Estimation of Total Power

Parametric value of window glass heating or room

The following table 5.1 shows the recommended Parametric value of glass heating or room determined from existing data and numerical result for determination of total power needed on defogging period and sizing the component of storage. For instance the duct exit area is determined according to the simulation case study.

Table 5.1.Parametric value of glass heating or room

Density of air (kg/m^3)	1.2
Side glass duct Exit area (m^2)	0.00204
Windshield glass duct exit area (m^2)	0.004
Initial glass and room temperature (K)	266
glass or room heating temperature (K)	303
Specific heat pressure constant (Cp)	1.005
All three port duct exit air velocity (m/s)	6
Static Pressure at cold flow (pa) @71cfm	106
Inlet portion of the duct area (m^2)	0.0034
Inlet portion of the duct air velocity (m/s)	14 or2756 FPM
Volumetric floret of inlet portion of the duct (m^3/s)	0.0337 or 71cfm
Safety Factor (k) assumed that from 1-3 range	1.3

Consider a three widow glass is heated with air at a maximum temperature 37°C. The room and widow glass initial temperature is -6°C. The required air flow rate can be calculated as

$$P = Av\rho C_p(T_h - T_c) = (2As + Aw)v\rho C_p(T_h - T_c) = 1.4kw \quad (15)$$

Where A is total exit area of designed duct

A_s is exit area of side glass ducts

A_w is exit area of windshield glass ducts

$$A = 2As + Aw$$

V is Inlet portion of the duct air velocity

$$P_T = P + \mathrm{AHP} = V(m^3/s)\rho C_p(T_h - T_c) + \mathrm{AHP} \tag{16}$$

for

$$\mathrm{AHP} = \frac{\mathrm{CFMx}(\mathrm{SP} + \left(\frac{\mathrm{FPM}}{4005}\right)^2)}{6356} = 0.38HP = 0.3kw$$

$$P_T = P + \frac{\mathrm{CFMx}(\mathrm{SP} + \left(\frac{\mathrm{FPM}}{4005}\right)^2)}{6356} \tag{17}$$

$$P_e = VI = kP_T = 1.176(0.3 + 1.4\ ) = 2\mathrm{kw}$$

5.4.1 Standard Air Duct Selection for prototype

From the theory of fluid flow the better duct shape and branches has selected based on the design of defogger flow distribution into three entities right side widow, windshield, and left side window. The selected configuration is on appendix I.

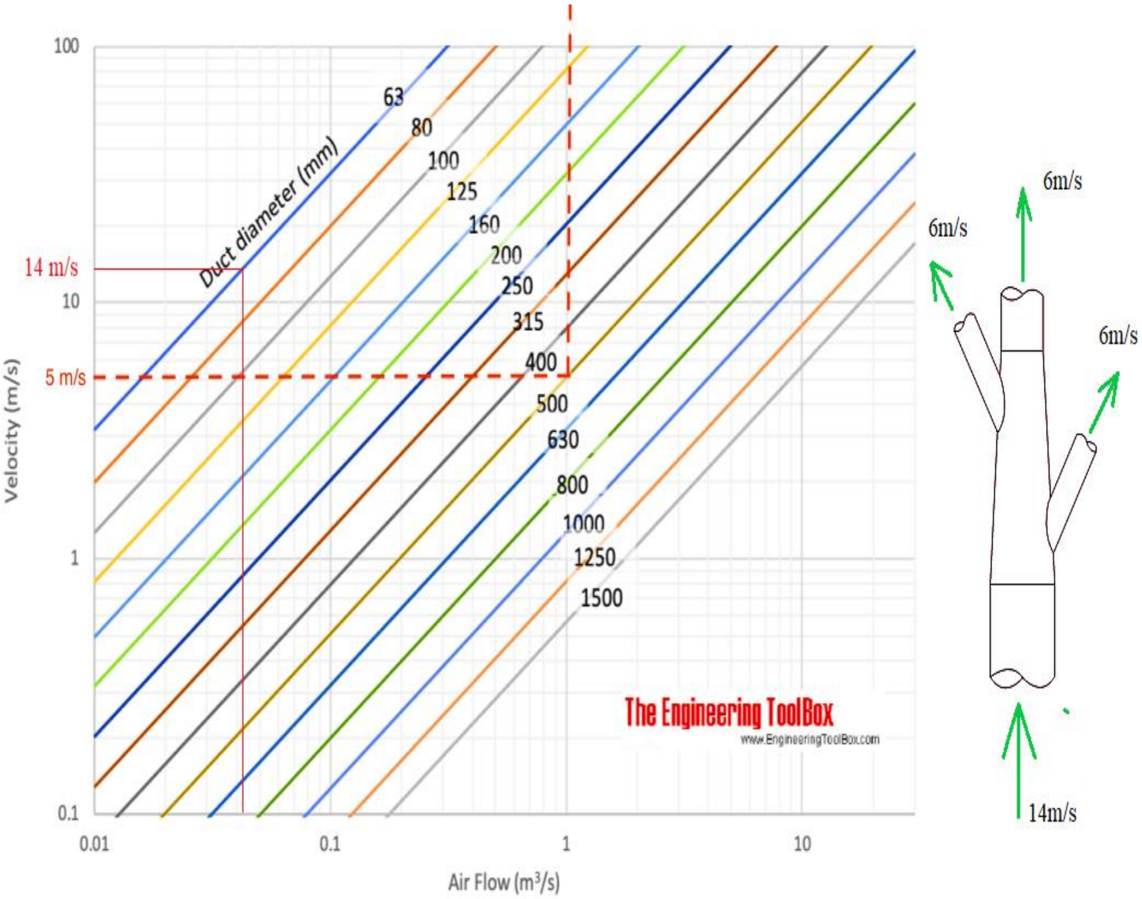

Figure 5.1.Air Ducts - Friction Loss Diagram

5.5 Selection of battery

Lead acid batteries are the most usually used type of battery in photovoltaic systems. Although lead acid batteries have a low energy density, only moderate efficiency, and high maintenance requirements, they also have a long lifetime and low costs compared to other battery types. One of the singular advantages of lead acid batteries is that they are the most commonly used form of battery for most rechargeable battery applications (for example, in starting car engines), and therefore have a well-established established, mature technology base.Therefore, for this work considering also solar energy the selected battery is Lead acid battery. Lead acid battery is shown in figure 5.2.

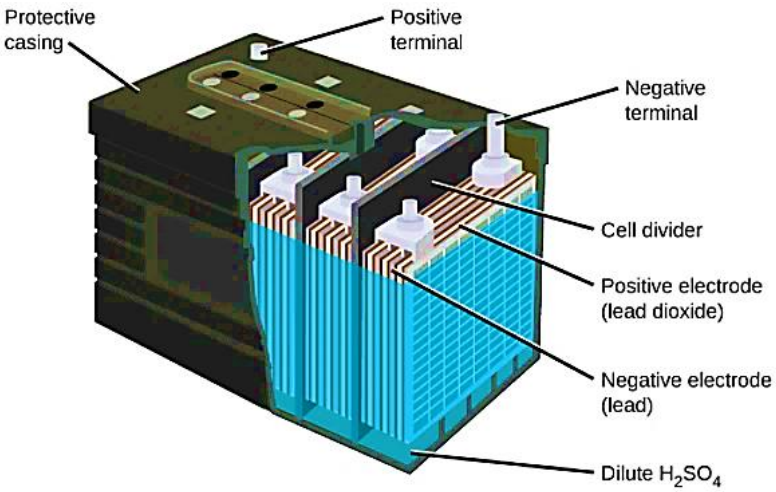

Figure 5.2.Lead acid Battery Features (www.atbatt.com)

Constant current discharge curves for a 120 Ah lead acid battery at different discharge rates, with a limiting voltage of 1.85V per cell (Mack, 1979). Longer discharge times give higher battery capacities.

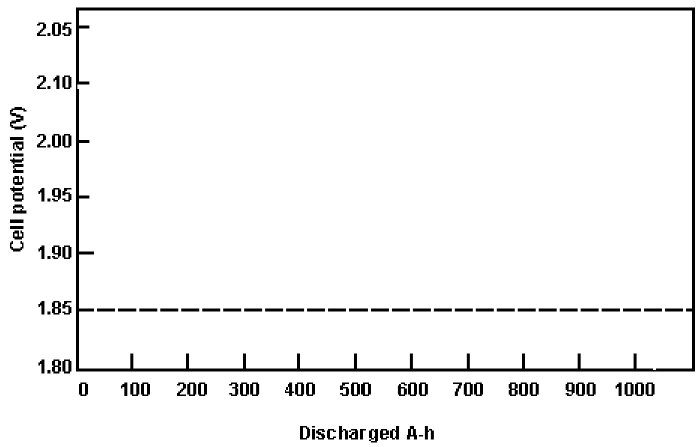

Figure 5.3.Discharging level of lead acid batter (www.atbatt.com)

Operation of Lead Acid Batteries

A lead acid battery consists of a negative electrode made of spongy or porous lead. The lead is porous to facilitate the formation and dissolution of lead. The positive electrode consists of lead oxide. Both electrodes are immersed in a electrolytic solution of sulfuric acid and water. In case the electrodes meet each other through physical movement of the battery or through changes in thickness of the electrodes, an electrically insulating, but chemically permeable membrane separates the two electrodes. This membrane also prevents electrical shorting through the electrolyte. Lead acid batteries store energy by the reversible chemical reaction shown below.

5.5.1 Summary and Comparison of Battery Characteristics

There are a large number of battery parameters. Depending on which application the battery is used for, some parameters are more important than others. The following is a list of parameters that may be specified by a manufacturer for a given type of battery. For example, in a typical battery for a general car, the energy density is not relevant - a battery is a small fraction of the total battery weight and consequently this parameter would typically not be listed for a conventional car battery. However, in electric vehicle applications, the battery weight is a significant fraction of the overall weight of the vehicle and so the energy densities will be given.

Installation

Battery installation should be conducted in accordance with the relevant standard in the country in which they are being installed. At present, there are Australian standards AS3011 & AS2676 for battery installation. There is also a draft standard for batteries for RAPS applications which will eventually become an Australian standard.

Among other factors to be considered in the installation of a battery system are the ventilation required for a particular type of battery bank, the grounding conditions on which the battery bank is to be placed, and provisions taken to ensure the safety of those who may have access to the battery bank. In addition, when installing the battery bank care must be taken to ensure that the battery temperature will fall within the allowable operating conditions of the battery and that the temperature of the batteries in a larger battery bank is at the same temperatures. Batteries in very cold conditions are subject to freezing at low states of charge, so that the battery will be more likely to be in a low state of charge in winter. To prevent this, the battery bank may be buried underground. Batteries regularly exposed to high operating temperatures may also suffer a reduced lifetime.

5.5.2 Battery Sizing

For the same reason, an estimated factor is used to roughly estimate a battery's Ah rating for long or short time periods.

- For a runtime of less than 2 hours, a factor of 1.5 is used.
- For a runtime of over 2 hours, a factor of 1.3 is used.

The above factor is for lead-acid batteries. For AGM batteries, possible to use 1.05–1.15 and for Gel batteries, 1.10–1.25 can be used.

Battery size can be deduced by using a couple of formulae. First, we need to calculate the load current and then we need to multiply it by the runtime factor

- Load = 2000W *(has been calculated using from previous guide)*
- Input volte = 12V
- Required Runtime = 0.5hours
- UPS Efficiency/Power Factor = 70% or 0.7 (this should be used if you don't want to estimate it)
- Battery type = Lead-Acid (So runtime factor of 1.5)

Load Current for 1 hour = (Runtime Factor x Load) / (UPS Efficiency x UPS Input) = 1.5 x 2000/ (0.7*12) = 240A

Load Current for 1 hours = Answer x 1 = 238 x 0.5 = 119Ah

Now that we know our current usage for 0.5 hour, calculating the battery size is easy. We need battery size of 120Ah. The nearest round number is 120Ah.

5.5.3 Battery Charging Voltage

For it is possible to determine the number of cells required can be determined more precisely in order to match with the load tolerance more accurately. The number of battery cells expected to be linked in series fashion must fall between the two limits which are minimum and maximum. Maximum number of cells required to be connected in series:

$$N_{maximum} = \frac{V_{dc}(1 + V_{load,\,max})}{V_{charging}} = \frac{12x(1 + 0.20)}{2.25} = 7$$

Minimum number of cells required to be connected in series:

$$\mathrm{Nminimum} = \frac{\mathrm{Vdc}(1 + \mathrm{Vload,min})}{\mathrm{Veodv}} = \frac{12x(1 - 0.1)}{1.8} = 7$$

Where

$N_{maximum}$, Maximum battery cells required

$N_{minimum}$, Minimum battery cells required

V_{dc}, Battery Voltage (Nominal)

$V_{load,min,}$ Minimum load voltage tolerance in %

$V_{load,max}$ Maximum load voltage tolerance in %

V_{eodv}, Represents end of discharge voltage (V_{dc})

$V_{Charging}$, charging voltage of cell (V_{dc})

$V_{max} = N_{maximum} V_{charging} = 7x2.25 = 15.75v$

$V_{min} = N_{minimum} V_{eodv} = 7x1.8 = 12.6v$

5.5.4 Charger Size of Sized lead acid Battery

To select the recommended charger for sized lead acid battery. The manufacturers have already listed the lead acid battery for different ampere hour that used for charging. From the appendix IV the charger needed for charging this lead acid battery is described as follow.

	Voltage	charger	battery	
Schumacher-SP1	6 or 12 v	2 or 4 Ah	10-120Ah	all lead acid

5.6 Invertor used for Defogger machine

The power invertor is the basic use of converting the low voltage 12v DC to high voltage 120 AC in order to drive the machine through AC Power. These devices can provide normal house current from a variety of 12-volt DC (direct current) sources, including your automobile lighter. When coupled with a bank of batteries, voltage inverters are used in battery backups for computers and other electronic equipment. Therefor considering the total power needed for blowing and heating element 2000W the portable defogging machine take AC voltage using the invertor from 12Volt DC.

5.6.1 Invertor size determination Step

Because for fan and heater resistor assemblies takes AC power

Step 1

To determine the power consumption (wattage) of the device wished to operate. The wattage of a device is commonly listed either in the owner's manual, or on a label affixed to the device. For multiple devices add all wattages together. This is 2000w

Step 2

Procure a voltage inverter which is rated to supply the number of watts you will need. There are several types of inverters. For power requirements are 2000 watts. Inverters with a larger capacity are available, but they require a direct wired connection to your battery.

Step 3

It should verify that, DC power source is sufficient to power the inverter and attached devices.

Generally, every 10 watts of power consumption will require one amp of DC current to be supplied. It is to be verified that the batteries can supply this much current and the circuit breakers or fuses are sufficiently sized.

Step 4

Connecting the voltage inverter to DC source. This can be as simple as plugging the device into a cigarette lighter, or by connecting it to one or more 12-volt batteries. If connecting to batteries, use battery terminal connectors appropriate for the battery type found. Using wire strippers to expose an inch of bare conductor at the ends of the power inverter's DC input wires. Connect each wire to the proper battery terminal, being careful not to mix positive and negative connections.

5.7 Size of Solar Panel to Charge 12V

For a 100 watt, solar panel is a common solar panel size any one could use to charge some of the most common 12V battery capacities. However, if there is a big battery, to charge it quickly, it will likely need to buy multiple solar panels and connect them together to create a solar panel array. From appendix VI, it has been sized that, the solar panel size that need to store 12v 120 Ah battery size is 440watt charged with PWM Controller. Therefore, in order to reach battery load power it should be around five number of solar panel with this selected size. However, it is possible to charge up to single panel size which is 440watt to consider only for necessity of short time defogging. The following figure shows the components used for battery solar charging system.

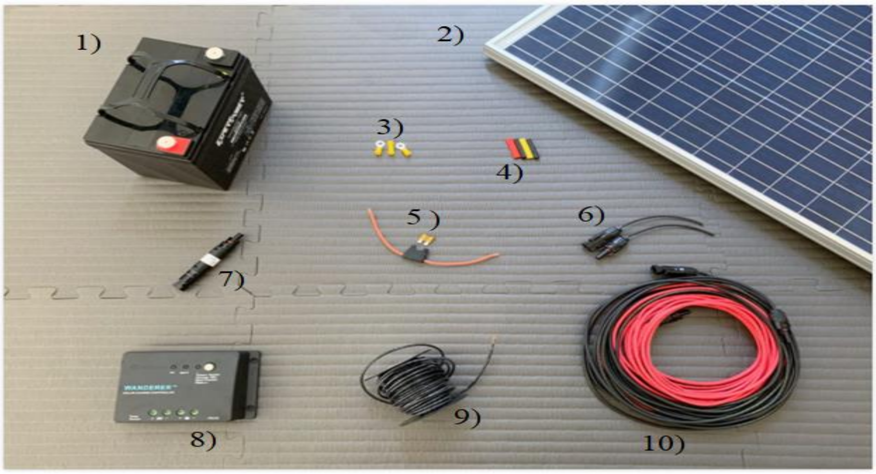

Figure 5.4.solar powers with Battery components

1. Battery, 2. Solar panel, 3. Connector, 4, 5, 6 sockets 7. Tester, 8. Controllers PWM. 9, 10 are wire

5.7.1 Multiple Solar Pannel Circuit Diagram

Around two reasons to use diodes in a solar panel. Generally, the PN Junction diodes are used in solar panels. The first reason is to bypass the current. The diode used in solar panel to bypass the current is called **Bypass Diode**. The Bypass Diode is connected in parallel and reverse bias with an individual solar panel when a number of solar panels are used together. In case, if any panel is damaged or sun rays not properly reach that solar panel then the bypass diode works and bypasses the current. It is possible to see in the figure 5.5, the solar panel A is damaged, so in this case, the bypass diode connected with the solar panel A resolve bypass the current.

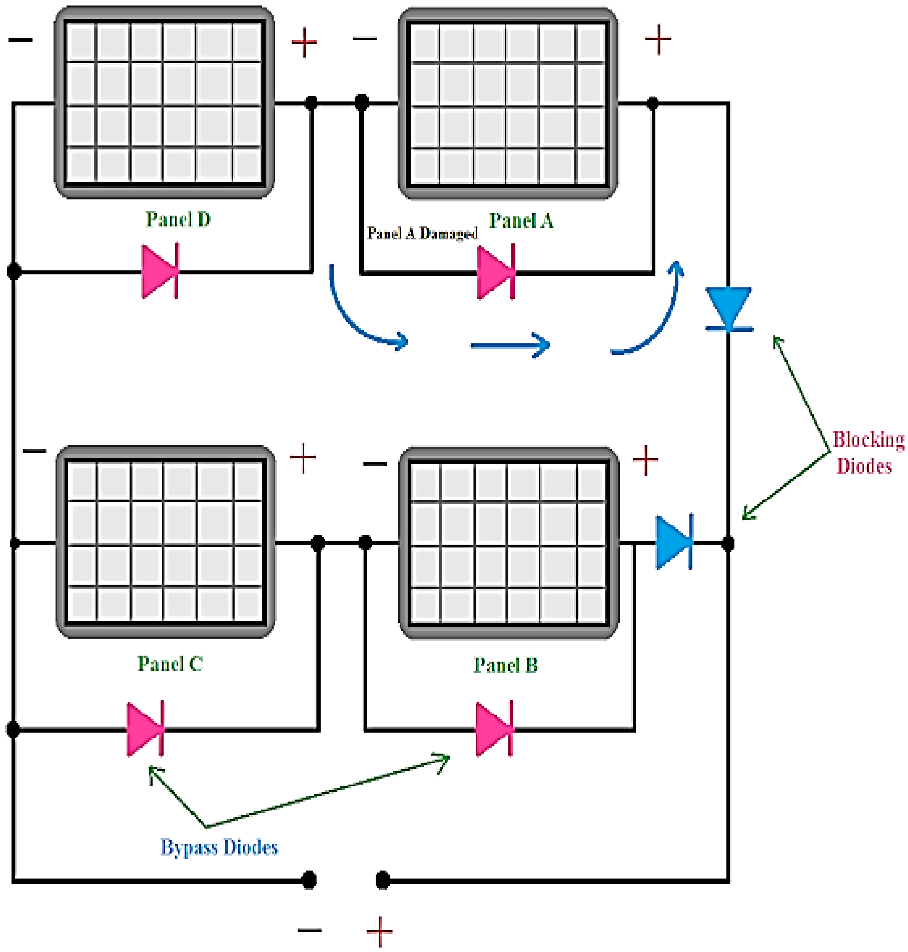

Figure 5.5.Multiple solar powers assemble with Battery

The **Blocking Diode is used in Solar Panel** to block the opposite power flow. Suppose we connect a solar panel to a battery for charging. When the solar panel getting, proper sun rays it creates sufficient voltage to charge the battery and in this case, the current begin to flow from the solar panel to the battery. However, when the sun rays decrease, then the solar panel create lower voltage than the battery and current flow from the battery to the solar panel.

Therefore, the Blocking Diode prevents the current flow from the battery to the solar panel. The Blocking Diode also prevents the current flow from one string of panels to another string.

5.7.2 Final Defogger Machine for Manufacturing

The model and the drawing of the final defogger machine is shown in figure 5.6

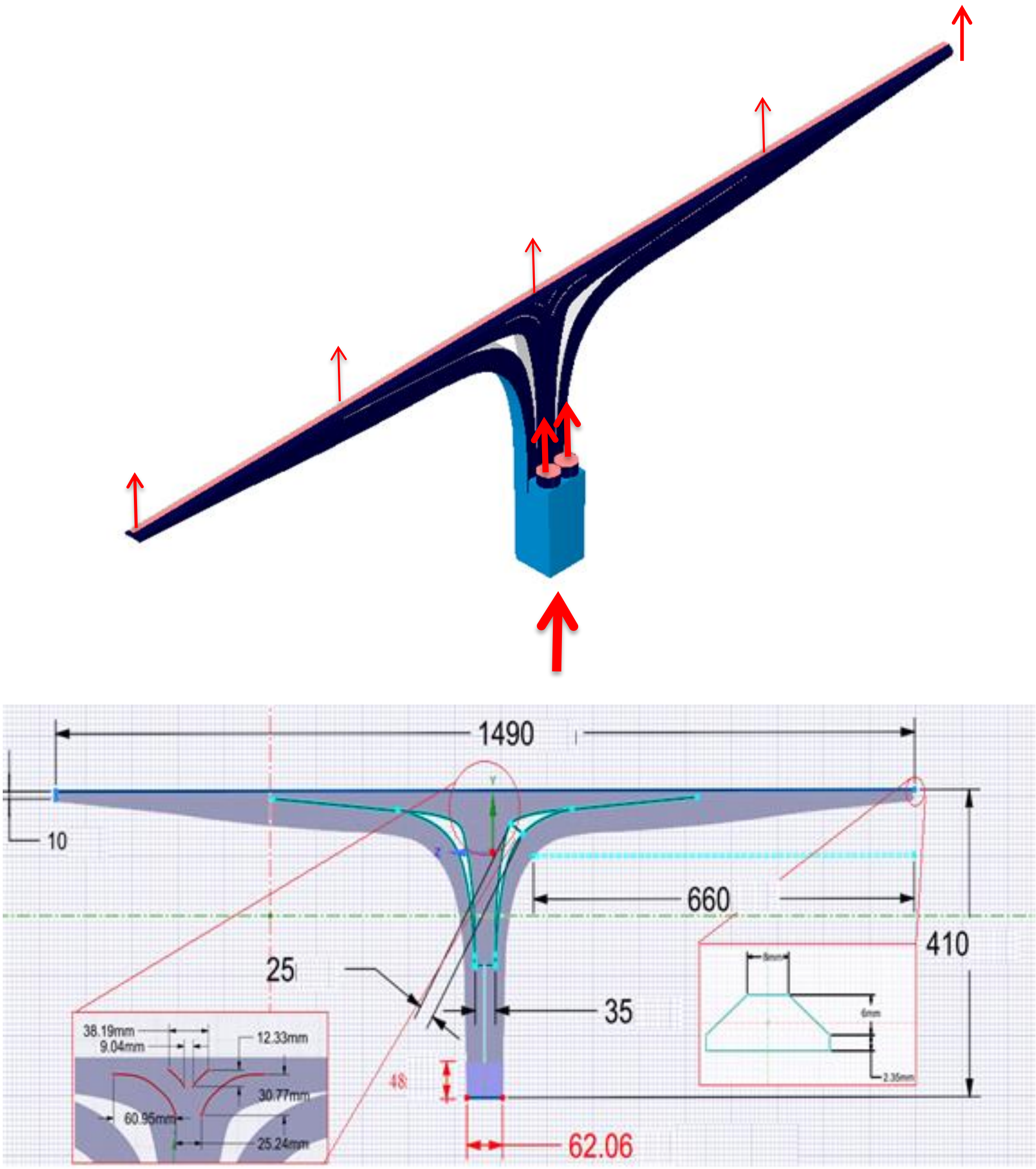

All dimensions are in millimeters

Figure 5.6.Final Defogger Machine for Manufacturing

5.8 Organized Material for Prototype

Hose and Defogger wall Material

A flexible high temperature hose is an important piece of equipment, providing extreme heat resistance and tight-bending flexibility. Therefor for this type of solicitation, flexible high temperature hose is an important. The material of both hose and defogger wall is PVC (Polyvinyl chloride) which is widely used in electrical cable construction for insulation, bedcovers, and casing. It is Eco-friendly and is non-*conductors* of electricity with absolute flame-retardant features that have Thermal behavior up to 210^{O}C.

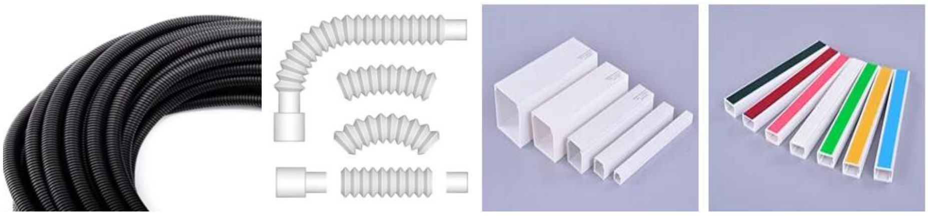

(a) (b)

Hose Defogger Wall

Figure 5.7. (a) Flexible hose and (b) electric conduit

Portable Electric Fun and Resistor

It is known that the designed defogger machine is portable on energy consumption sides which total electric power is around 2000W. Therefore in order to consider both electric fun and air heater element the verily approached simplified model of a heat gun hot air blows out machine components are used to get the main circuit board, fun with resistor and others control switches. A heat gun emits concentrated heat that can burn defogger system wall. Therefore, it is impossible to use directly. Means there must be mounted diverging flow nozzles that take the flow from the converged nozzle of source term to the defogger inlet portion. On the other hand, it is possible to change the temperature of the heating air. Because of three variable temperatures, change is present which start from 50-400 degree Celsius. Total power consumption is 2000W.

(a) (b) (c)

Figure 5.8. (a) Turbo Fan with heating element, (a) Motor with Fan and (c) heating element

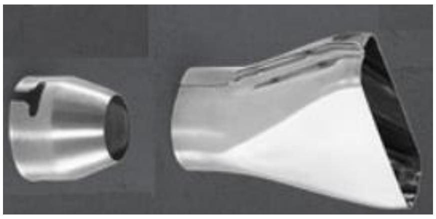

Figure 5.9.Converging and diverging nozzle

5.9 Prototyping Provision Steps

On this research, work even if the numerical design has been made for three window glasses windshield, right and left window on driver compartment area, the prototype has been limited to both side window glasses for the designed shape of defogger is the same for all glass windows. This is to test flow divided equal for both side window glass. The following steps are followed for the prototype.

Step 1

Molding rectangular box that used as hot air duct distributor from gesso for one inlet port and three exitports to link defogger machine of two side window glass and windshield. Because gesso has ability to sustain the concentrated temperature.

(a)

Step 2

Assembling the exit port of distributor box with defogger connector white hose

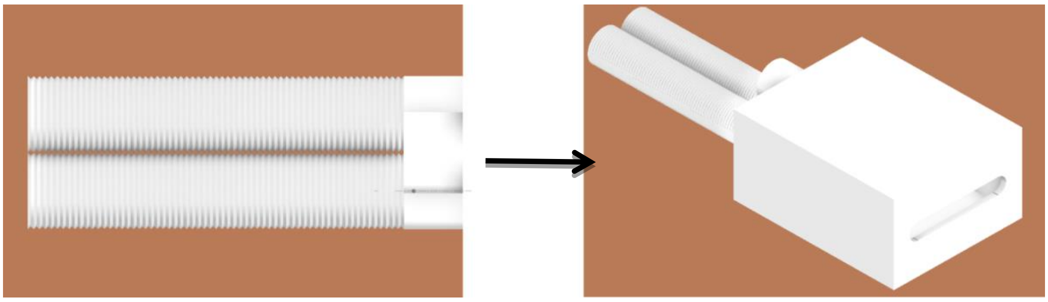

(b)

Step 3

Painting

Black paints absorb light, so it is better that the white body painted with black is well good on improvement for driver visibility to minimize the reflection from box surface. There for the defogger hot air distributor box or duct divider should be black rather than white.

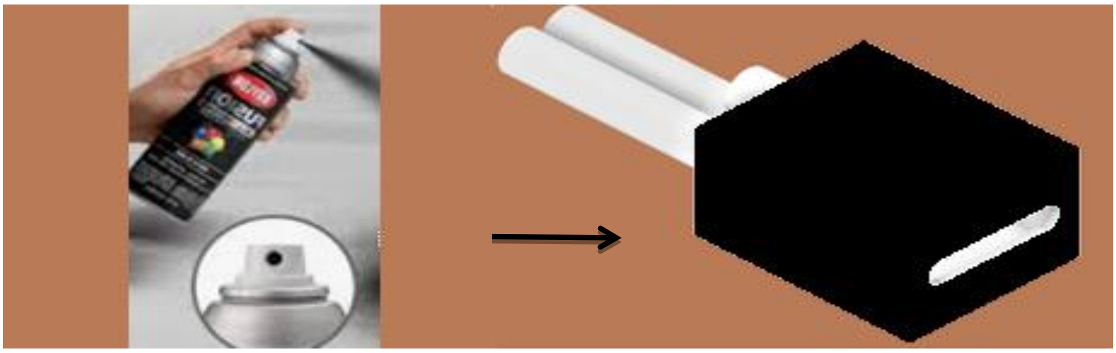

(c)

Step 4

On this step the connecting white hose with black or discharge black flexible hose that linked with side window Deffoger wall is organized as follow.

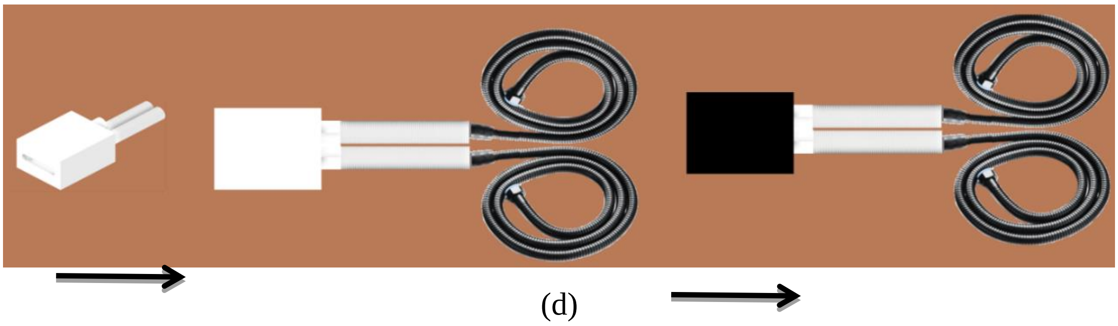

(d)

Step 5

Side window Deffoger wall

(e)

Step 6

Full assemble of turbo fan and heating element with hot air distributor box and deffoger wall

(f)

Step 7

Full assemble with 6volt battery

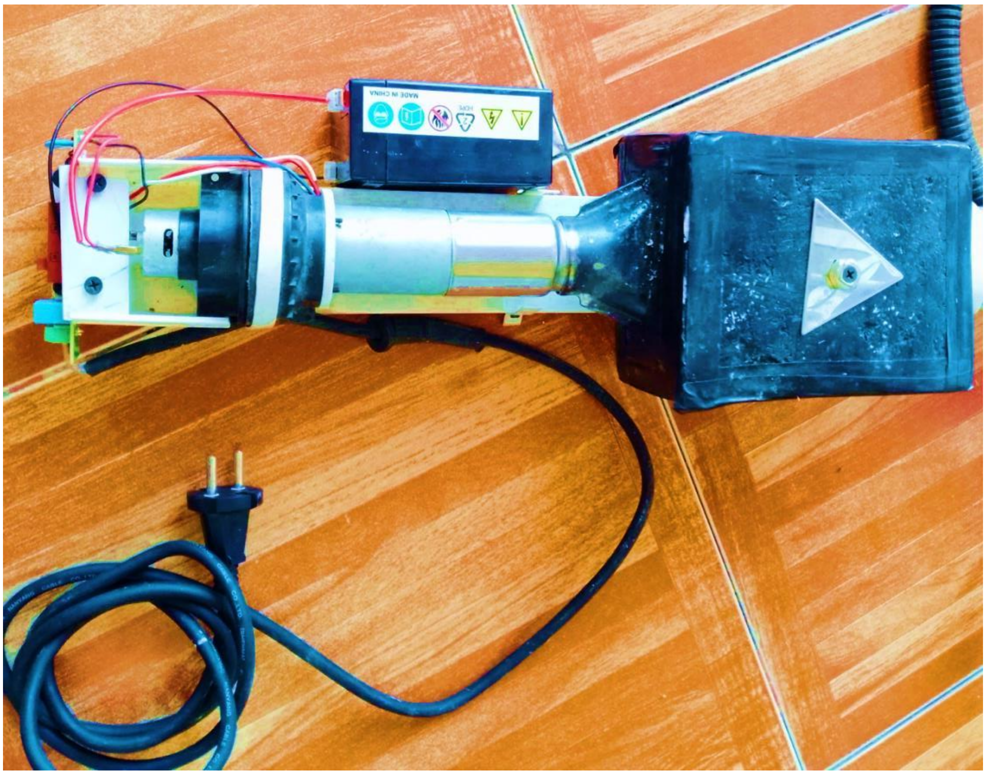

(g)

(h)

Figure a,b,c,d,e,f,g and h Component of machine

5.10 Cost Estimation of Prototyped Machine

Thetotal cost estimation of prototype fabrication for portable Defogger is determined as the following table below.

Table 5-2.Total Prototype cost

Name	Unit	Unit Price	Cost (Birr) ETB
White hose	2	200	400
Black hose	2	200	400
Gesso (Gypssum)	2	12.5	25
Heating Element with Turbo Fan	1	3500	3500
Spray Paint	1	600	600
PVT , Electric cable Conduit	1	100	100
Fabrication , Equipment and labour cost	5days	1000	5000
Battery (6v.4.5Ah)	1	650	650
		Total Cost	**10,675**

CHAPTER SIX
SUMMARY OF RESULTS

6.1 Summary

In this investigation, CFD is used to simulate vehicle defogger and side window glass flow and heat transfer to determine the velocity field and contours of defogged pattern in terms of the liquescent portion of ice. FLUENT with a defogging model based on the temperature is used in the simulation. The results provided a perception into the characteristics of the flow and defogger performance. Based on the melting pattern, it is concluded that the performance of the current nozzle design meets requirements.

Simulation results are offered in terms of the flow track lines, velocity field, and liquid fraction contours of the ice. These results are showed in Figures. They prove the general direction of the flow as it departures the duct nozzle and disseminates throughout the compartment. The maximum velocity is approximately 6 m/s near the nozzle exit and reduces to about 1.0 m/s along the upper of the window glass. The velocity diminishes as the flow moves up along the window glass inner surface. There is a pattern of flow deflection to the sides near both ends of the nozzle. It is evident that, in general, the velocity decreases as the flow propagates into the interior compartment away from the window glass.

The Numerical simulation of the automobile defogs process with a full scale model and comparison with standard value of Federal state which verifies the numerical results. Because there are reports of poor visibility from mist and fog on drivers to notice the calls for safety in the weather and road conditions. The novel idea on this research work, the defogger duct nozzle is designed based on standardized boundary condition of automobile defogging in laboratory experiment by means of the Federal Motor Vehicle Safety Standards (FMVSS) used in U.S. and Society of Automotive Engineering SAE. In this investigation, Computational Fluid Dynamics (CFD) is used to numerically simulate vehicle defogger performance. The general-purpose CFD package Ansys fluent is used to perform the numerical simulation. The first stage of simulation is about portable duct design that used to distribute the flow in exit port equally. On duct flow design, cold air with the steady state performance under the turbulence model of k-epsilon is simulated. The final shape of the duct nozzle is accepted as prime design. Later the duct design is completed, it becomes bring together with vehicle side window and wind shields to study numerical simulation of the automobile defoger process with a full scale Toyota HIECE 2004 quarter model. The simulation is performed by assigning multiphase flow model with Eulerian wall film. The liquid film thickness is applied to the window glass according to the experimental results from previous work of average non-movable liquid water film of 315.4 μm and 337.2 μm based on diode laser absorption spectroscopy (DLAS) and Ultrasonic pulse-echo method (UPEM) measurement recorded respectively. The hot air velocity is injected from the exit portion of duct to the film surfaces on the glass windows. In order to investigate the effect of film wall thickness on defogging time, the film thickness 0.35mm, 0.7mm, 1.05mm, and 1.4mm are simulated. The special parameter predicted on here is volume fraction of water film varied after certain flow time. For all four different film thicknesses, the defogging performance simulation takes a time 1500, 2500, 3000 and 3500second respectively to remove all condensed water from the surface. Finally, the best option for this research work to design ShowTime defogging that have no longer to stay the ice on the surface. There for the selected film thickness for highly portables for three windows is considered as 1500 second film thickness, which is 0.35mm. The designee followed 1500sec to size the heater, fun, and battery for selection criteria. Then prototype has been made for demonstration and its functionality. The operationally of prototype is already justified that the prototype has been demonstrated.

CHAPTER SEVEN
CONCLUSIONS AND RECOMMENDATIONS

7.1 Conclusion

From the general summary, the drawn results are based on simulation performed by assigning a multiphase flow model with Eulerian wall film. The film thickness is applied to the surface by making the liquid water film as 315.4 μm and 337.2 μm based on diode laser absorption spectroscopy (DLAS) and the Ultrasonic pulse-echo method (UPEM) measurements recorded respectively. As the hot air is injected, velocity is injected from the exit portion of the duct to the film surfaces on the glass windows. The special parameter is predicted as the volume fraction of the water film changes after a certain flow time. For four different film thicknesses, 0.35mm, 0.7mm, 1.05mm, and 1.4mm, the defogging performance simulation takes a time of 1500, 2500, 3000, and 3500 seconds, respectively, to remove condensed water from the surface. Finally, the best option for this work applied to design shows time defogging that has no longer to stay the ice on the surface. Therefore, the selected film thickness for high portables for three windows is considered as 1500 second film thickness, which is 0.35mm. The designee followed 1500sec to size the heater, fan, and battery for selection criteria. The prototype is made for demonstration and its functionality. Finally, by looking the operational principle of prototype reference to numerical designed defogger it is possible to design the portable defogger that is used to remove the foggy from all three windows on passenger cars.

7.2 Recommendation

The recommended terms are used to know for all users of this document. Numerical simulation can be successfully used to analyze an automobile defogging system, and CFD can be a very useful design tool for an automobile air conditioning system. Subsequently, using computer simulations, it is possible to derive the time-based development of the window glass.

In this way, it is possible to modify the ducts and outlet configurations in the defogger system and predict the performance of the modified system. Additionally, as it is already described in the results as the operational attitude of prototype guided by numerical designed defogger, this can justify the possibility of designing the portable defogger using numerical analysis before any manufacturing activity.

7.3 Future Work

- The air driving out of the de-ice duct onto the window glass is lightly non uniform; this may provide, resulting in the non-uniform temperature on the window glass. So further improving for this, the flow distribution on window glass is good.
- In the future scope, the researchers can check the numerical analysis of newly designed portable defoggers on large duty and some public buses. To form the acceptability of the designed defogger shape on other vehicles.
- It is know that even the present designed defogger power source is from battery, it needs to use the invertor for the changing DC toAC current that feed to defogger. This makes the defogger work on AC Supply. The future researcher could consider the Direct DC current for defogger machine from battery.

REFERENCES

Taro Ono et al (2019), Analysis of Defogging Performance, Thermal Comfort, and Energy Saving for HVAC System Optimization in Passenger Vehicles. EDP Sciences (2019).

A Ene, C Teodosiu (2021). Studies dealing with defogging and de-icing phenomena on vehicles' windshield: a review. IOP Conf. Series: Earth and Environmental Science 664 (2021) 012071

FMVSS 103, "Windscreen defrost and defog systems", Federal Motor Vehicle Safety Standard CFR Part 571, Vol. 77, No. 4, (2012).

FMVSS 104, "Windshield wiping and washing systems", Federal Motor Vehicle Safety Standard -49 CFR Part 571, Vol. 77, No. 4, (2012).

Aroussi, A., Hassan, A., Clayton, B., AbdulNour, B. and Rice, E., "Improving vehicle windshield defrosting and demisting", (2012), SAE Technical Paper.

Wang, M., Urbank, T.M. and Sangwan, K.V., "Clear vision" automatic windshield defogging system", (2016), SAE Technical Paper.

Karamjit, S., "Simulation of the windscreen defrost performance", in Star European User Conference., (2011).

Skea, A.F., et al. (2016), "Comparison of CFD simulation methods and thermal imaging with windscreen defrost pattern", (2016), SAE Technical Paper.

Aroussi, A. and Aghil, S. (2017), "Characterisation of the flow field in a passenger car model", Optical Diagnostics in Engineering, Vol. 4, No. 1, (2017), 1-15.

Zolet, A., "CFD and experimental correlation of the defrost flow and vehicle windshield defogging", in 21 the Brazilian Congress of Mechanical Engineering, Natal, RN, Brazi., (2011).

Croce, G., et al. (2007) "Numerical simulation of windshield defogging process", Proceedings of the Institution of Mechanical Engineers, Part D: Journal of Automobile Engineering, Vol. 221, No. 10, (2007), 1241-1250.

R.B. Kharat, et al (2007). Modeling of in cabin climate and fogging windshield SAE Technical paper, 2007-01-0767

Jixuan Liu, ET AL (2016)“Analysis of Maximum Return Air Ratio on No-Fogging Condition by In-cabin Climate Simulation of EV (2016)

Himanshu.et al (2014). "Feasibility study and development of refrigerator cum air conditioner", International Journal of Scientific and Research Publications, Vol. 4, No. 12, (2014), 1-6.

Tehertovskaia, N.(2018), "Simulation model for the climate at the windshield of a passenger car compartment", (2018).

S. J. Kang, et al (2011). Automobile Defrosting System Analysis Through A Full-Scale Model. International Journal of Automotive Technology, Vol. 12, No. 1, pp. 39−44 (2011)

ZhilongHe , et al (2020). Analysis and Optimization of Truck Windshield Defroster. Appl. Sci. 2020, 10, 5671; doi: 10.3390/app10165671

MaciejGis, et al (2021). Efficiency of electric vehicle interior heating systems at low ambient temperatures. https://doi.org/10.1515/eng-2021-0006

Hyu-Goo Kang et al (2008). The study of defrosting performance on automobile Windshield through different injection angle. 대한기계학회 2008 년도추계학술대회논문집

Arafat A. Bhuiyan and Jamal Naser (2017). Development of 3D transient wall filming mechanism during combustion by coupling Eulerian-Lagrangian approach and particle-wall interaction model. Applied Thermal Engineering. www.journals.elsevier.com/applied-thermal-engineering

E.M. Papoutsis–Kiachagias and K.C. Giannakoglou (2014), Continuous Adjoin Methods for Turbulent Flows, Applied to Shape and Topology Optimization: Industrial Applications. Archives of Computational Methods in Engineering, DOI 10.1007/s11831-014-9141-9, 2014.

Dohyung Kim et al (2020). Improvement of Defogging Performance of Automobile Defroster using Vortex Generators. Springer-Verlag GmbH Germany, part of Springer Nature 2020

HuinanYang , et al (2018). Measurement of liquid water film thickness on opaque surface with diode laser absorption spectroscopy. School of Energy and Power Engineering, University of Shanghai for Science and Technology, No. 516, Jungong Road, Yangpu District, 200093 Shanghai, China

E.M. Papoutsis–Kiachagias, et al (2015), Noise Reduction in Car Aerodynamics using a Surrogate Objective Function and the Continuous Adjoint Method with Wall Functions. Computers and Fluids, 122, pp. 223-232, 2015.

E.M. Papoutsis–Kiachagias, et al (2014), Applied to Shape and Topology Optimization: Industrial Applications. Archives of Computational Methods in Engineering, DOI 10.1007/s11831-014-9141-9, 2014.

E.M. Papoutsis–Kiachagias (2013), Adjoin Methods for Turbulent Flows, Applied to Shape or Topology Optimization and Robust Design. PhD Thesis, NTUA, 2013.

I. Goldasteh, et al (2015), Numerical Simulation of Airflow Distribution on the Automobile Windshield in Defrost Mode. SAE Technical Paper 2015-01-0330, doi:10.4271/2015-01-0330, 2015.

W. Yang, et al (2012), Flow Field Simulation, and Performance Analysis of HVAC Defrosting Duct. 2nd International Conference on Electronic & Mechanical Engineering and Information Technology (EMEIT-2012), China, 2

E.M. Papoutsis–Kiachagias, et al (2015), The Continuous Adjoin Approach to the k–e Turbulence Model for Shape Optimization and Optimal Active Control of Turbulent Flows. Engineering Optimization, 47 (3), pp. 370-389, 2015.
E.M. Papoutsis–Kiachagias, et al (2015), Noise Reduction in Car Aerodynamics using a Surrogate Objective Function and the Continuous Adjoint Method with Wall Functions. Computers and Fluids, 122, pp. 223-232, 2015.
Manuel Lorenz (2015), Reduction of Heating Loads and Interior Window Fogging in Vehicles.Die Dissertation wurde am 09.06.2015 beider Technischen Universität München eingereicht

Peng KE, Jie LIU, Yi LU (2019). Modeling and analysis the thin wall film formation with integrated discrete and continuous phase simulation approach. School of Transportation Science and Engineering, Beihang University 16^{th} – 18^{th} September, 2019

APPENDIX

Appendix I: air ducts - friction loss diagram

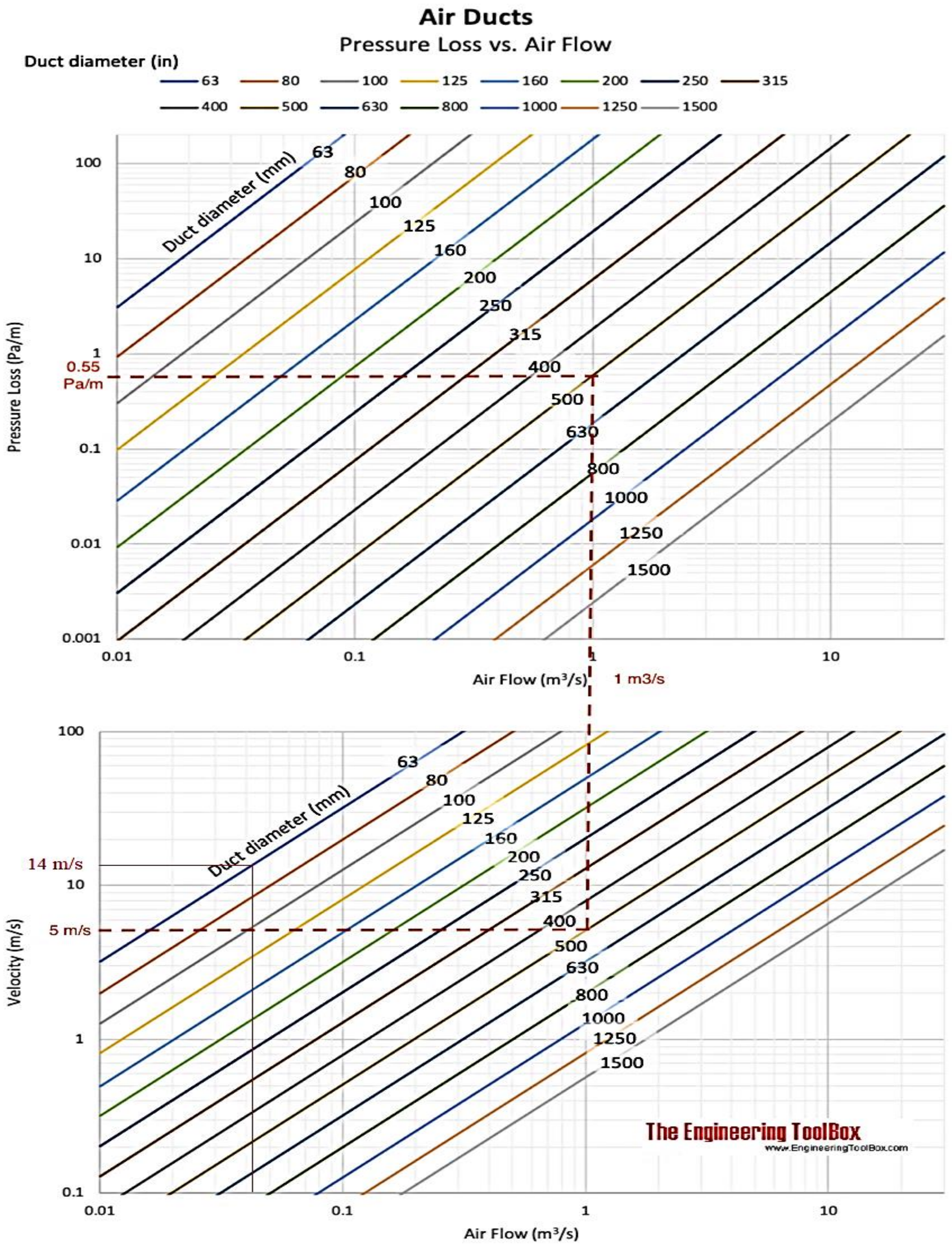

Appendix II: Summary and Comparison of Battery Characteristics

Specifications	Lead Acid	NiCd	NiMH	Li-ion		
				Cobalt	Manganese	Phosphate
Specific energy density (Wh/kg)	30–50	45–80	60–120	150–190	100–135	90–120
Internal resistance[1] (mΩ)	<100 12V pack	100–200 6V pack	200–300 6V pack	150–300 7.2V	25–75[2] per cell	25–50[2] per cell
Cycle life[4] (80% discharge)	200–300	1000[3]	300–500[3]	500–1,000	500–1,000	1,000–2,000
Fast-charge time	8–16h	1h typical	2–4h	2–4h	1h or less	1h or less
Overcharge tolerance	High	Moderate	Low	Low. Cannot tolerate trickle charge		
Self-discharge/ month (room temp)	5%	20%[5]	30%[5]	<10%[6]		
Cell voltage (nominal)	2V	1.2V[7]	1.2V[7]	3.6V[8]	3.8V[8]	3.3V
Charge cutoff voltage (V/cell)	2.40 Float 2.25	Full charge detection by voltage signature		4.20		3.60
Discharge cutoff voltage (V/cell, 1C)	1.75	1.00		2.50 – 3.00		2.80
Peak load current Best result	5C[9] 0.2C	20C 1C	5C 0.5C	>3C <1C	>30C <10C	>30C <10C
Charge temperature	–20 to 50°C	0 to 45°C		0 to 45°C[10]		
Discharge temperature	–20 to 50°C	–20 to 65°C		–20 to 60°C		
Maintenance requirement	3–6 months[11] (topping chg.)	30–60 days (discharge)	60–90 days (discharge)	Not required		
Safety requirements	Thermally stable	Thermally stable, fuse protection common		Protection circuit mandatory[12]		
In use since	Late 1800s	1950	1990	1991	1996	1999

Appendix III: Battery selection characteristics

NO.	ITEMS	VOLTAGE	CAPACITY C_{10}	DIMENSION(mm)				GROSS WEIGHT	TERMINAL
	NO	VOLT	AH/10HR	Length	Width	Height	Total Height	(KGS)	TYPE
1	6-GFM-33G	12	33	196	131	155	180	10	F3
2	6-GFM-38G	12	38	198	166	170	170	12.1	F3
3	6-GFM-40G	12	40	198	166	170	170	13.7	F3
4	6-GFM-55G	12	55	229	138	210	228	15.2	F4
5	6-GFM-65G	12	65	348	168	178	178	21.1	F4
6	6-GFM-75G	12	75	260	168	209	227	23.8	F4
7	6-GFM-90G	12	90	307	169	208	227	28.5	F4/F8
8	6-GFM-100G	12	100	329	172	214	243	31.5	F4/F8
9	6-GFM-120G	12	120	409	177	207	234	35.3	F9
10	6-GFM-150G	12	150	483	170	240	240	44.2	F4/F10
11	6-GFM-200G	12	200	522	240	218	223	60.1	F5/F11
12	6-GFM-250G	12	250	522	268	218	223	66	F5/F11
13	GFM-200G	2	200	170	110	330	350	14.3	F7
14	GFM-300G	2	300	171	151	330	366	20.3	F7
15	GFM-400G	2	400	211	176	329	367	27	F7
16	GFM-500G	2	500	241	172	330	365	32.1	F7
17	GFM-600G	2	600	301	175	331	366	39.1	F7
18	GFM-800G	2	800	410	176	330	365	48.1	F7
19	GFM-1000G	2	1000	475	175	327	365	64.2	F7
20	GFM-1200G	2	1200	475	175	327	365	71	F7
21	GFM-1500G	2	1500	401	351	342	378	101	F7
22	GFM-2000G	2	2000	491	351	343	383	132	F7
23	GFM-3000G	2	3000	712	353	341	382	192	F7

Appendix IV: charger size for different lead acid battery (https://www.atbatt.com/)

SKU	Voltage	Charger Ah	Recommended Battery Capacity	Recommended Battery Type
021-0127	6	0.75	1.2-40Ah	SLA, VRLA, AGM, Deep Cycle, Gel Cell, LiFePO4
021-0144	6	1.25	10-95Ah	SLA, VRLA, AGM, Deep Cycle, Gel Cell, LiFePO4
021-0152	8	1.25	10-95Ah	SLA, VRLA, AGM, Deep Cycle, Gel Cell, LiFePO4
021-0123	12	0.75	1.2-40Ah	SLA, VRLA, AGM, Deep Cycle, Gel Cell, LiFePO4
022-0150-DL-WH	12	0.8	1.5-40Ah	Waterproof: SLA, VRLA, AGM, Deep Cycle, Wet, Flooded,Conventional (best for ATVs, watercraft, motorcycles, or boats)
021-0128	12	1.25	10-95Ah	SLA, VRLA, AGM, Deep Cycle, Gel Cell, LiFePO4
021-0156	12	1.25	10-95Ah	Gel Cell
022-0148-DL-WH	12	1.25	10-95Ah	International: SLA, VRLA, AGM, Deep Cycle, Wet, Flooded,Conventional
022-0165-DL-WH	12	1.25	10-95Ah	International: SLA, VRLA, AGM, Deep Cycle, Wet, Flooded,Conventional
021-0133	12	2	10-155Ah	SLA, VRLA, AGM, Deep Cycle, Gel Cell, LiFePO4
021-0134	12	2	10-155Ah	SLA, VRLA, AGM, Deep Cycle, Gel Cell, LiFePO4
021-0147	12	2	10-155Ah	SLA, VRLA, AGM, Deep Cycle, Gel Cell, LiFePO4
022-0142-DL-WH	12	5	10-215Ah	International: SLA, VRLA, AGM, Deep Cycle, Wet, Flooded,Conventional

022-0157-1	12	5	10-215Ah	Waterproof: SLA, VRLA, AGM, Deep Cycle, Wet, Flooded,Conventional (best for ATVs, watercraft, motorcycles, or boats)
021-1158-12	12	20	45-215Ah	Heavy Duty: SLA, VRLA, AGM, Deep Cycle, Wet, Flooded,Conventional
022-0158-1	24	2.5	10-215Ah	SLA, VRLA, AGM, Deep Cycle, Wet, Flooded,Conventional, LiFePO4
022-0169	36	15	45-215Ah	Golf Cart Battery Charger - Also ok for Industrial SLA, VRLA, AGM, Deep Cycle, Wet, Flooded,Conventional
022-0170	48	10	45-215Ah	Golf Cart Battery Charger - Also ok for Industrial SLA, VRLA, AGM, Deep Cycle, Wet, Flooded,Conventional (SLI, Marine, RV)
GEN1	12	10	25-230Ah	Waterproof: SLA, VRLA, AGM, Deep Cycle, Wet, Flooded,Conventional (best for boats, tractors, powersports)
G7200-1	12 or 24	7.2	14-230Ah	Recovers slightly sulfated batteries. SLA, VRLA, AGM, Deep Cycle, Wet, Flooded,Conventional (best for Motorcycle, ATV, Jet Ski or Snowmobile batteries - can also charge SLI, RV or boat)
G26000	12 or 24	26	25-500Ah	Deep Cycle (best for Motorcycles, ATV, UTV, Snowmobile, Jet Ski, SLI, RV, Boat, Truck)
GEN2	12 to 24	10	25-230Ah	Waterproof: SLA, VRLA, AGM, Deep Cycle, Wet, Flooded,Conventional
GEN3	12 to 36	10	25-230Ah	Waterproof: SLA, VRLA, AGM, Deep Cycle, Wet, Flooded,Conventional
GEN4	12 to 48	10	25-230Ah	Waterproof: SLA, VRLA, AGM, Deep Cycle, Wet, Flooded,Conventional
G750	6 or 12	0.75	1.2-30Ah	SLA, VRLA, AGM, Deep Cycle, Wet, Flooded,Conventional (best for Motorcycle, ATV, Jet Ski or Snowmobile

				batteries - can also charge SLI, RV or boat)
G1100	6 or 12	1.1	2.2-40Ah	SLA, VRLA, AGM, Deep Cycle, Wet, Flooded,Conventional (best for Motorcycle, ATV, Jet Ski or Snowmobile batteries - can also charge SLI, RV or boat)
G3500	6 or 12	3.5	1.2-120Ah	SLA, VRLA, AGM, Deep Cycle, Wet, Flooded,Conventional (best for Motorcycle, ATV, Jet Ski or Snowmobile batteries - can also charge SLI, RV or boat)
LC-2195	6	0.3	1-3Ah	SLA, VRLA, AGM, Deep Cycle, Gel Cell, LiFePO4
LC-2200	6	1	3.3-10Ah	SLA, VRLA, AGM, Deep Cycle, Gel Cell, LiFePO4
LC-2211	6	4	13.3-40Ah	SLA, VRLA, AGM, Deep Cycle, Gel Cell, LiFePO4
LC-2199	12	0.3	1-3Ah	SLA, VRLA, AGM, Deep Cycle, Gel Cell, LiFePO4
LC1-12-1A	12	1	3.3-10Ah	SLA, VRLA, AGM, Deep Cycle, Gel Cell, LiFePO4
LC1-12-3A	12	3	10-30Ah	SLA, VRLA, AGM, Deep Cycle, Gel Cell, LiFePO4
PSC-12500A	12	0.5	2-5AH	SLA, VRLA, AGM, Deep Cycle, Gel Cell, LiFePO4
PSC-124000A-C	12	4	20-40Ah	SLA, VRLA, AGM, Deep Cycle, Gel Cell, LiFePO4
PSC-1210000A	12	10	8-20Ah	SLA, VRLA, AGM, Deep Cycle, Gel Cell, LiFePO4
PSC-241000A-C	24	1	5-10Ah	SLA, VRLA, AGM, Deep Cycle, Gel Cell, LiFePO4
Schumacher-SE-1-12S	12	1.5	10-230Ah	Best for use on RV, deep cycle, SLI, heavy duty that may have long storage period

Schumacher-SSC-1500A	12	2,10,15	10-300Ah	gel, wet flooded all sla DEEP CYCLE SLI HEAVY DUTY
Schumacher-SSC-1000A	12	2,6,10	10-230Ah	gel, wet flooded all sla DEEP CYCLE SLI HEAVY DUTY
Schumacher-SP2	6 or 12	1	2.2-40Ah	all lead acid
Schumacher-SEM-1562A	6 or 12	1.5	10-95Ah	gel, wet flooded all sla DEEP CYCLE SLI HEAVY DUTY
Schumacher-SP3	6 or 12	3	10-120Ah	all lead acid - motorcycle/SLI/RV/Boat
Schumacher-SP1	6 or 12	2 or 4	10-120Ah	all lead acid
Schumacher-CR-2	6 or 24	1.5	TOY	Battery powered ride-on toys
Schumacher-SP-200				Solar Battery Maintainer
Schumacher-SP-400				Solar Battery Maintainer
Schumacher-SP-1500				Solar Battery Maintainer
Schumacher-SPC-7A				Solar Charge Controller - Protects batteries and panels
UPG-D1730	12	0.5	1.25-5Ah	SLA, VRLA, AGM, Deep Cycle, Gel Cell, LiFePO4
BM-24041	24	4	10-120Ah	maintenance-free, marine, deep cycle, sealed, gel, and all popular brands of AGM dry-type
SHO-BMS01	6 or 12	2		Shorai LFX SERIES

Appendix V: Specific heat of air at 1 bar (= ElifSomuncu 2018)

Temperature			Isochoric specific heat (Cv)					Isobaric specific heat (Cp)				
[K]	[°C]	[°F]	[kJ/mol K]	[kJ/kg K]	[kWh/(kg K)]		[kcal(IT)/(lb °F)]	[kJ/mol K]	[kJ/kg K]	[(kW h)/(kg K)]	[kcal(IT)/(kg K)] [Btu(IT)/lb °F]	[kcal(IT)/(lb °F)]
60	-213	-352	0.03398	1.173	0.0003258		0.2287	0.05506	1.901	0.000528	0.45405	0.37071
78.79	-194	-318	0.03044	1.051	0.0002919		0.205	0.05599	1.933	0.000537	0.46169	0.37695
81.61	-192	-313	0.02172	0.75	0.0002083		0.1463	0.03154	1.089	0.000303	0.2601	0.21237
100	-173	-280	0.02109	0.728	0.0002022		0.142	0.03012	1.04	0.000289	0.24833	0.20276
120	-153	-244	0.02093	0.7225	0.0002007		0.1406	0.02953	1.022	0.000283	0.2435	0.1993
140	-133	-208	0.02081	0.7184	0.0001996		0.1401	0.02937	1.014	0.000282	0.24219	0.19774
160	-113	-172	0.02077	0.7172	0.0001992		0.1399	0.02928	1.011	0.000281	0.24147	0.19716
180	-93.2	-136	0.02076	0.7166	0.0001991		0.1397	0.0292	1.008	0.00028	0.24076	0.19657
200	-73.2	-99.7	0.02075	0.7163	0.000199		0.1397	0.02917	1.007	0.00028	0.24052	0.19638
220	-53.2	-63.7	0.02075	0.7163	0.000199		0.1397	0.02914	1.006	0.000279	0.24028	0.19618
240	-33.2	-27.7	0.02075	0.7164	0.000199		0.1397	0.02914	1.006	0.000279	0.24028	0.19618
260	-13.2	8.3	0.02076	0.7168	0.0001991		0.1398	0.02914	1.006	0.000279	0.24028	0.19618
273.2	0	32	0.02077	0.7171	0.0001992		0.1398	0.02914	1.006	0.000279	0.24028	0.19618
280	6.9	44.3	0.02078	0.7173	0.0001993		0.1399	0.02914	1.006	0.000279	0.24028	0.19618
288.7	15.6	60	0.02078	0.7175	0.0001993		0.1399	0.02914	1.006	0.000279	0.2403	0.1962
300	26.9	80.3	0.0208	0.718	0.0001994		0.14	0.02915	1.006	0.00028	0.24036	0.19625
320	46.9	116	0.02083	0.7192	0.0001998		0.1403	0.02917	1.007	0.00028	0.24052	0.19638
340	66.9	152	0.02087	0.7206	0.0002002		0.1405	0.02923	1.009	0.00028	0.241	0.19677
360	86.9	188	0.02092	0.7223	0.0002006		0.1409	0.02926	1.01	0.000281	0.24123	0.19696
380	107	224	0.02098	0.7243	0.0002012		0.1412	0.02931	1.012	0.000281	0.24171	0.19735
400	127	260	0.02105	0.7266	0.0002018		0.1417	0.02937	1.014	0.000282	0.24219	0.19774
500	227	440	0.0215	0.7424	0.0002062		0.1448	0.02983	1.03	0.000286	0.24597	0.20083
600	327	620	0.02213	0.7641	0.0002123		0.149	0.03044	1.051	0.000292	0.25103	0.20496
700	427	800	0.02282	0.7877	0.0002188		0.1536	0.03114	1.075	0.000299	0.25675	0.20963
800	527	980	0.02351	0.8117	0.0002255		0.1583	0.03183	1.099	0.000305	0.26249	0.21432
900	627	1160	0.02415	0.8338	0.0002316		0.1626	0.03247	1.121	0.000311	0.26772	0.21858
1100	827	1520	0.02525	0.8716	0.0002421		0.17	0.03356	1.159	0.000322	0.27675	0.22596
1500	1227	2240	0.02673	0.923	0.0002564		0.18	0.03505	1.21	0.000336	0.28901	0.23597
1900	1627	2960	0.02762	0.9535	0.0002649		0.1859	0.03593	1.241	0.000345	0.29631	0.24193

Appendix VI: 12V 120Ah lead acid batterySolar Panel Size

Charge Time	Charge Controller Type	Est. Solar Panel Size
5 peak sun hours	MPPT	350 watts
10 peak sun hours	MPPT	130 watts
15 peak sun hours	MPPT	90 watts
20 peak sun hours	MPPT	60 watts
25 peak sun hours	MPPT	50 watts
5 peak sun hours	PWM	440 watts
10 peak sun hours	PWM	170 watts
15 peak sun hours	PWM	110 watts
20 peak sun hours	PWM	80 watts
25 peak sun hours	PWM	60 watts